FRONT PAGE

PROJECT FINAL REPORT

Grant Agreement number: 304842

Project acronym: NANOBIO4TRANS

Project title: A new nanotechnology-based paradigm for engineering vascularised liver tissue for transplantation

Funding Scheme: FP7-CP-FP

Period covered: **from** 1 September 2012 **to** 31 August 2015

Name of the scientific representative of the project's co-ordinator[1], Title and Organisation:

Professor Jenny Emnéus, DTU Nanotech

Tel: +45 4525 6867

Fax: +45 4588 7762

E-mail: jenny.emneus@nanotech.dtu.dk

Project website Error! Bookmark not defined. **address:** http://www.nanobio4trans.eu/

[1] Usually the contact person of the coordinator as specified in Art. 8.1. of the Grant Agreement.

4.1 Final publishable summary report

4.1.1. Executive summary

NanoBio4Trans has merged hiPSC-, perfusable hybrid scaffolds (PHS)- and biosensor technologies to develop new tools to be used in biomedical research beyond the present state-of-the-art. The outcome has been the development, optimisation and validation of a highly vascularised *in vivo*-like BAL as a potential extracorporeal bioartificial liver, ready to be perfused with human blood plasma. The BAL has been characterised and its metabolic capability and other essential functions (e.g. clearance of ammonia, bilirubin, toxins and bile acids) has been assessed. Precision-cut liver slices (PCLS) incubated in Liver-on-a-Chip systems has been used together with new LC-based bioassays for quality control of the newly engineered tissue.

Major steps have involved: (1) Fabrication of PHS with different geometries and porosities. (2) Exploration of *in vitro* cellular systems for development of 3D cell/tissue culture systems starting from hiPSCs, using perfusion based BAL-on-a-Chip systems for 3D perfusion culture, and further adaptation for potential up-scaling to larger size BAL support system to form BALs in the order of cm^3 to dm^3. (3) Comparison and validation of the developed fluidic BAL-on-a-Chip system with fluidic Liver-on-a-chip, containing precision-cut liver slices (PCLS) obtained from surgical waste from transplant, used as the gold standard to which the BAL systems have been compared.

Novel strategies to make 3D scaffolds with microporous *structured*, *random*, and *combined structured/random* channel network architecture have been achieved, using a combination of 3D filament printing of sacrificial moulds, polymer casting and sugar/salt leaching procedures, realising woodpile and hexagonal scaffold architecture. *Nanostructured interpenetrating networks (IPNs)* of hydrogel deposits inside these 3D scaffolds have been achieved, which has made it possible to deliver a drug that specifically can activate gene expression in cells residing in the interior of the 3D scaffolds. The developed strategy allows scaling up of scaffold size in dm^3 and in principle larger scale, the main challenge being the availability of enough cells for seeding inside.

Scaling up of hiPSCs production through 3D spheroid cultures has successfully been realised, and freezing procedures for easy transport of cells/spheroids to partners. Defined medium for the expansion of undifferentiated hiPSCs and differentiation in an optimised culture system with achieved mature hepatocytes with increased CYP-activities and CYP-induction function has been achieved. The developed protocols towards hepatocyte protocols are very robust, and more than 28 cell lines have been tested for their ability to grow undifferentiated as well as successful differentiation into not only hepatocytes but also other cell types (lung- and beta cell progenitors). State-of-the art maturity and functionality of hepatocytes and hepatospheres derived from hiPSCs has been achieved.

Two types of BAL support systems have been developed: (1) 16-bioreactor array intended for improved throughput optimization experiments of cell culture and differentiation conditions. (2) 8-bioreactor array incorporating needle-electrodes for bioimpedance analysis of real time cell proliferation in 3D over time. Efficient operation of the BAL support system requires precise control of their key physical, chemical and physiological parameters. To implement this, advanced optochemical- and electrochemical sensors and assays have been developed and applied for monitoring hiPSC-derived liver tissue and human precision cut liver slices (PCLS). The human BAL was moreover assessed and compared to human PCLS. Various functions, such as Phase I and II metabolism, synthesis, as well as expression of hepatic genes responsible for liver development, metabolism, synthesis and transport, were tested. This is the first time that the function of hiPSC-derived hepatocytes has been compared to fresh human tissue, and it revealed that these hiPSC-derived human hepatocytes cultured under the applied conditions show as yet unrivalled functionality, with excellent comparability of liver functions with fresh liver tissue.

4.1.2. Project context and objectives

4.1.2.1. Project context

Organ transplantation has been a major scientific and clinical breakthrough in the 20th century, in spite of many associated problems, such as lack of organ donors and/or rejection of the transplanted organs and life-long heavy medication with side effects. The innovative therapeutic approach of the 21th century is focusing on bioartificial organs to circumvent present problems, using a multidisciplinary and complementary approach to achieve the targeted goals. Tissue engineering and stem cell biology have uncovered groundbreaking opportunities for cellular re-programming, i.e., some cell types can be changed into a pluripotent stem cell (**PSC**) by over-expressing key transcription factors. These, so called induced pluripotent stem cells (**iPSC**)[1] share the two key characteristics with embryonic stem cells (**eSC**): self-renewal and pluripotency (i.e. they can differentiate to form any cell type in the human body). Crucially they are generated from adult cells circumventing many ethical concerns associated with using human eSC. Tander the discovery of human iPSC (**hiPSC**) enables the growth of an almost unlimited supply of a patient´s own cells, potentially conferring the ability to grow and regenerate tissues and organs[2] from 'self', which is envisaged to resolve many organ rejection[1, 3] related issues. Similarly, recent developments in material science and nanobiotechnology have produced engineered materials and devices that can be manipulated and controlled by physical and chemical means, resulting in unique functional or analytical properties. The fusion of these fields with resulting synergistic effects will open up yet unexplored scientific possibilities. By involving SMEs with relevant and leading expertise in key scientific fields, NanoBio4Trans has taken an additional step forward, by transferring the scientific results into exploitation phase, focusing on a new paradigm for creating a bioartificial liver **(BAL)**.

4.1.2.2. Project objectives

NanoBio4Trans set out to create a new paradigm to engineer cutting-edge *scalable* highly vascularised BALs on the following hypotheses:

- The use of hiPSC as the starting material, is foreseen to enable the construction of personalised artificial organs from a patient´s own cells, which is expected to result in reduced organ rejection and increased availability of lifesaving organs for transplantation.
- Growth and differentiation into *in vivo*-like BALs is possible if hPSC-derived liver tissue is highly vascularised, i.e. penetrated with blood-vessel like channels lined with endothelial cells, and with immediate and nearby supply of the necessary growth factors and signalling molecules that support its growth and differentiation.
- Creation of novel scalable two-component perfusable hybrid scaffolds (**PHS**s).
- The use of integrated optical and electrical (bio)sensing systems for monitoring real time effects and changes during tissue growth will allow control and surveillance of BAL formation, with envisaged feed-back control.

In a short-term perspective (3 years), a personalised/patient specific liver seems unrealistic since it is very likely that the patient will already be dead before any hiPSC have been produced from a potentially liver deficient patient´s own cells to result in a BAL derived from these cells. In a long-term perspective (8-10 years), however, it is realistic to build libraries and biobanks with patient derived hiPSCs, as a first crucial step towards a patient specific BAL. **The main challenge will be to produce a fully functional BAL**. Researchers worldwide are attempting to develop artificial livers (**AL**s) and BALs in different ways, some of which are already in clinical testing[4]. So far, work is mainly focused on the creation of an extracorporeal liver for use as a liver support system (**LSS**) before an appropriate liver has been found for transplantation or until recovery of the patient´s own liver. In order to avoid immune rejection of the liver, the patient should ideally receive a transplant from somebody with an identical blood type (AB0 system). A more short-term step towards a BAL, less prone to rejection, may thus be to produce and store hiPSCs derived from individuals with different blood type from which blood type specific BALs could be produced.

By fusing hiPSC-, polymer hybrid scaffolds- and biosensor technologies new tools were developed for potential use in transplantation and biomedical research beyond present state-of-the-art. The final goal has been to develop, optimise and validate a highly vascularised *in vivo*-like BAL - as an extracorporeal bioartificial liver (**EBAL**) ready to be perfused with human blood plasma, to be exploited in the medical technology of the 21th century. Partner SMEs have a leading role in this process concerning both innovation and exploitation aspects.

NanoBio4Trans integrates PHS-, sensor- and hiPSC technologies into a **BAL support system** in which a highly vascularised BAL will grow under real time control and surveillance, as visualised in Fig. 1. This new concept is a vital step forward in future developments of personalised/patient specific liver for transplantation.

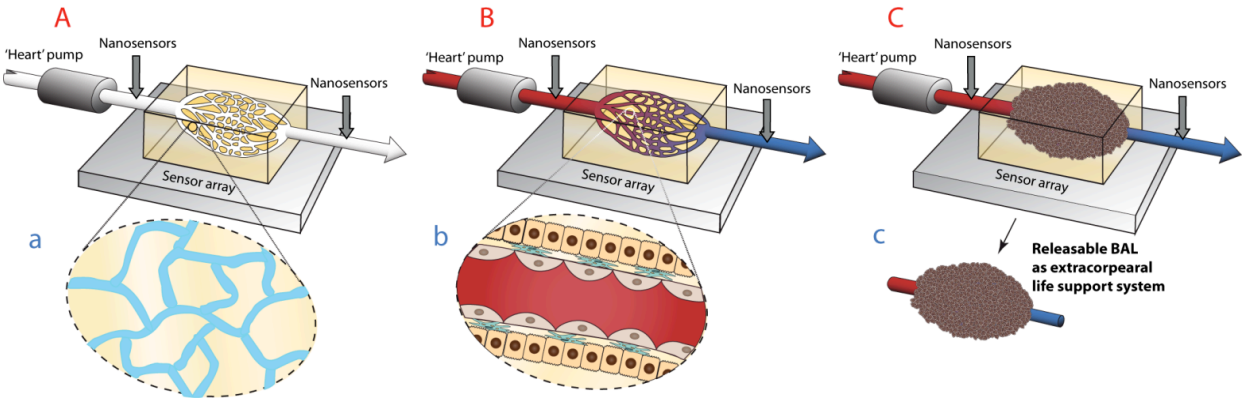

Figure 1. The NanoBio4Trans BAL support system´s development process: (A) The PHS with a highly branched perfusable channel network that allows flow through the material from one inlet to one outlet. (B) hPSC derived endothelial and hepatocyte cells seeded and grown inside the primary capillary channel network, to closely mimick the in vivo situation of blood vessel lined with endothelial cells on top of which hepatocyte monolayers are formed (Fig. 1Bb). (C) A fully developed BAL support system, with integrated sensing and imaging tools for control of growth and viability and use as EBAL, with a final releasable BAL (Fig. 1Cc), potentially for future transplantation (beyond project duration).

The NanoBio4Trans strategy has been to follow a step-by-step development of an increasing order of complexity, thus diminishing risks and assuring gain of knowledge beyond the state-of-the-art. Major steps are:

- To explore different *in vitro* cellular systems for development of novel 3D cell/tissue culture systems starting from (a) existing endothelial cells and moving on to (b) hiPSCs, as they have become available in the project, (c) using in a first instance miniaturised fluidic sensor array systems (**BAL-on-a-Chips**) for optimisation of 3D culture and perfusion conditions, and (d) further adaption for up-scaling to a large size BAL support system to form BALs in the order of cm^3 to dm^3.
- To compare and validate the developed BAL system with fluidic tissue slice sensor array systems (**Liver-on-a-chip**), containing precision-cut liver slices (**PCLS**) obtained from surgical waste from transplant. This reference system has been used as the gold standard to which the BAL systems will be compared.

4.1.3. Description of the main S&T results/foregrounds

4.1.3.1. Perfusable hybrid scaffold (PHS) technology

Summary

This activity has mainly been conducted in collaboration between DTU Nanotech and the SME Biomodics and has involved the development of scalable scaffold structures - **perfusable hybrid scaffolds** (**PHS**) - with highly dense capillary network, which serve as support for 3D growth and differentiation of hiPSC into a bioartificial liver (BAL) under perfusion control, as schematically illustrated in **Fig. 1A.**
The PHS development process involves a three-step procedure, i.e., formation of (1) *primary* highly branched perfusable microchannel network (structured fabrication processes) that allows flow through the material from one inlet to one outlet, and (2) a *secondary* more arbitrary random microporous network that connects the structured channels, and (3) a nanoporous *interpenetrating network (IPN)* that encloses hydrogel deposits of e.g. drugs, extracellular matrix proteins, differentiation factors, promoting hepatocyte adhesion, growth, differentiation and function. The created PHS has the following requirements and functions, where it should: (a) serve as structural and mechanical support for growth and differentiation of the BAL, (b) be perfusable with extensive channel networks that enable growth of blood vessels and transport of O_2 and nutrients to inner tissue and as a "nearby" source of important drugs and cell factors that sustains the growth of cells into a final BAL, and (c) be biocompatible and potentially biodegradable.

S&T results

A vast range of materials and methods were screened for their applicability to make random and structured porous scaffolds but also testing their biocompatibility. We developed a strategy to make primary structured scaffolds combined with secondary more arbitrary random structured in different materials and combination of materials, using the procedure described in **Fig. 2**.

Scalable **perfusable hybrid scaffold** (**PHS**) with highly dense capillary network and nanoporous hydrogel IPN deposits has been developed, which serve as support for 3D cell growth under perfusion control. The created PHS had two functions: mechanical support for growth of the BAL and as a "nearby" source of important cell factors and drugs that support the growth of cells into a final BAL. The final aim was to enable growth of cm^3 to dm^3 large highly vascularised BAL modules with high metabolic capacity.

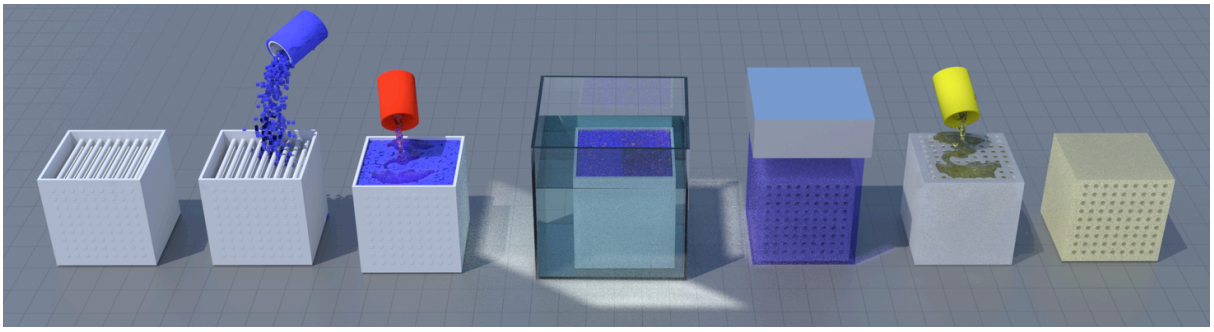

Figure 2. Procedure to make scalable combined structured and random porous PHS scaffolds: 1. Print PVA network defining larger channels (printed with a PVA shell). 2. Fill with salt/sugar (blue crystals). The PVA shell will keep the salt/sugar in place. 3. Add polymer elastomer solution (red liquid) and cure. 4. Dissolve salt/sugar and PVA network. (Here an additional treatment can follow, involving supercritical (sc) CO_2 treatment to introduce hydrogel IPN in the scaffold). 5. Plasma treatment of the scaffold. 6. Add extra cellular matrix (EMC) gels with cells (IPS cells, combinations of HUVECs/MSC etc.). 7. Cure gel and use!

The types of scaffolds we are able to fabricate today are:

- **Random porous channels**, created through the use of a random porous sugar or salt leaching proceedures. An ordinary random porous sugar cube can for instance be used as a mould,

encapsulated by an elastomer solution, which is cured around and inside the pores of the sugar. After polymer curing, the sugar is dissolved in water and removed, and an elastomer scaffold with random pores defined by the original pores of the sugar cube is the result.

- **Structured porous channels**, created through 3D printing of a sacrificial scaffold structure in e.g. polyvinyl alcohol (PVA). This scaffold is subsequently embedded in elastomer in the same way as described above for the sugar cube, and the sacrificial scaffold is dissolved and removed, creating a scaffold with structured channels defined by the 3D printed scaffold.
- **Combined structured and random channel networks - Dual pore scaffolds**, created through combining the two above procedures, as described in **Figure 3.**

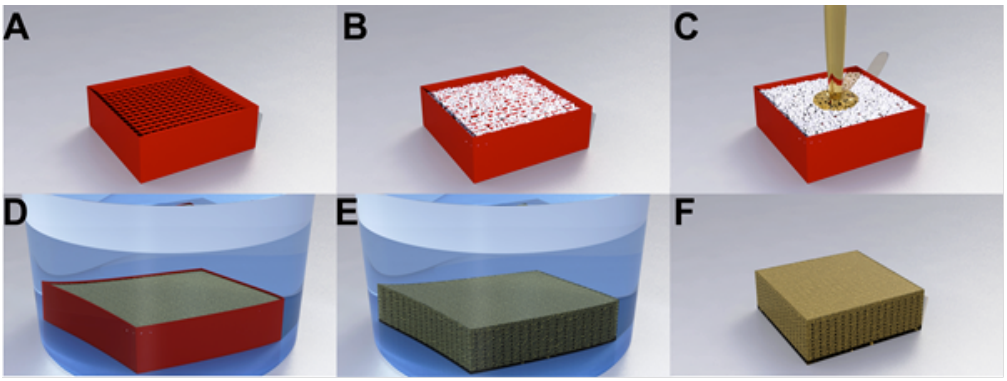

Figure 3. Fabrication of dual pore scaffolds: A sacrificial 3D mould was 3D printed in PVA (A) and packed with salt crystals (B). The salt-filled PVA mould was transferred into a container and PDMS was cast to cover it (C). Vacuum was applied to ensure complete filling of PDMS into the pores of the mould (D). Following crosslinking of the PDMS, the sacrificial PVA-salt mould was dissolved in water (E) releasing the dual-pore PDMS scaffold (F).

- **Hydrogel nano-deposit inside the dual pore scaffold – IPN scaffolds,** created through the introduction of interpenetrating polymer networks (IPN) of hydrogel using supercritical carbon dioxide **($scCO_2$),** as schematically illustrated in **Figure 4.** This is done through the swelling of the scaffolds in $scCO_2$ that contains hydrophilic monomer solution, optionally containing drugs or factors necessary for cellular growth and/or differentiation. The hydrophilic monomer solution is transported into the swollen elastomer and anchored through a free radical polymerization. In this way, an IPN of hydrogel nanodeposits and elastomer result in a PHS structure, capable of releasing different compounds (e.g. drugs, nutrient, growth factors). IPNs with different material combinations have been produced and tested. Especially the combination of silicone and a PEGylated acrylate, poly(ethylene glycol) methacrylate (pHEMA-PEGMEA)) have shown interesting properties.

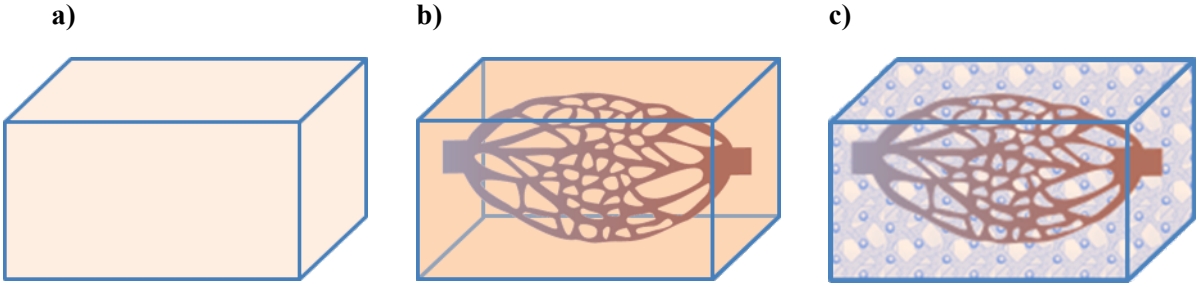

Figure 4. Illustration of the IPN scaffold concept, showing a) the base material, b) primary structured and/or random porous structure created within the base material, and c) a secondary IPN network within the PHS, enclosing hydrogel nano-deposits for *in situ* delivery of e.g. drugs, nutrients and growth factors.

Figure 5 shows the different types of scaffolds that have been created. PDMS (but also poly(ϵ-caprolactone) (**PCL**) and PHEMA) scaffolds with structured pores (**Fig. 5Ab**) were fabricated using 3D printed PVA filament moulds with woodpile pattern (**Fig. 5Aa**), while random pore scaffolds (**Fig. 5Bb**) were derived from cylindrical salt disks (**Fig 5Ba**). As shown in the SEM image of the structured pore scaffold in **Fig. 5Ac**, the pores are square shaped with dimension of ~ 400 µm × 400 µm and well

interconnected. In the random pore scaffolds the salt leaching process gives pores with dimensions in the range of 300-600 µm (**Fig. 5Bc**), as determined by the size distribution of the used salt crystals.

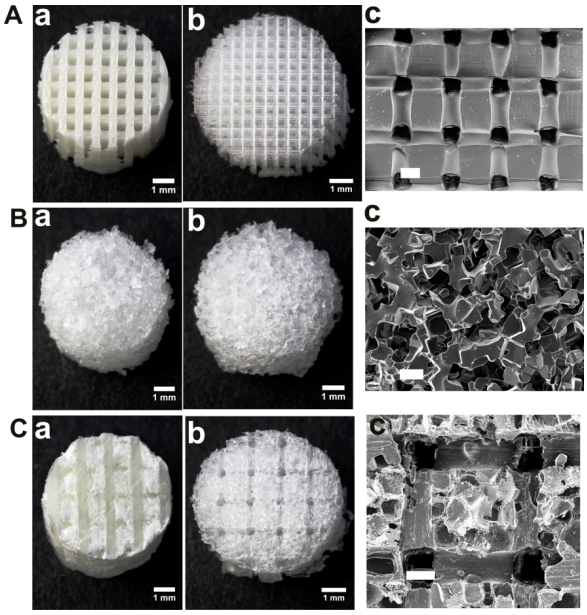

Figure 5. Sacrificial moulds and resulting fabricated porous PDMS scaffolds: A) 3D printed PVA mould (a) and replicated structured pore scaffold with pore size of 400 µm × 400 µm (b) and SEM magnification (c); B) photo of salt mould (a) and replicated random pore scaffold with pore size of 300-600 µm (b) and SEM magnification (c); C) photo of 3D printed PVA mould filled with salt (a) and replicated dual-pore scaffolds with structured pores of 400 µm × 400 µm and random pores of 300-600 µm (b) and SEM magnification (c). Scale bars: 1 mm in A, B and C (a & b); 400 µm in A, B and C(c).

By combining both approaches, we fabricated dual-pore scaffolds (**Fig. 5Cb**) with both defined structured and random pore microarchitectures, using the sacrificial 3D printed structured porous PVA filament moulds filled with salt crystals into the inter-filamentous space (**Fig. 5Ca**). The method of fabrication is simple and involves casting of the desired polymer in the mould, which specifies the microarchitecture of pores within the resulting scaffold. Surface top view of the dual-pore scaffold is shown in the SEM image in **Fig. 5Cc**. The structured pores of dimension ~400 µm × 400 µm are distributed in x, y and z directions, whereas the random pores with dimension of 300-600 µm are shown in between the structured pores of the bulk scaffold.

As shown in the SEM image of the top surface of a dual-pore scaffold in **Fig. 6A** and its zoom-in view **Fig. 6B (**schematically shown in **Fig. 6E**), the scaffolds have regular, well-structured and highly interconnected structured pores in the z (yellow lines) and x-y (red lines) direction throughout the scaffold. In between the structured pores, the scaffolds have an array of square shaped random porous regions of 800 µm × 800 µm. The salt crystals of size 300-600 µm fused together and generated large interconnected pores. **Fig. 6C** and its zoom-in **Fig. 6D**, show SEM image of cross-sectional view (**Fig. 6E**) of the interior of the scaffold. The channels in the scaffold have an elliptical cross-sectional profile, as the round PVA filament is flattened during printing of the mould, and the distance between two rows of structured pores is about 800 µm. The dimensions of the pores (width 344µm, height 190 µm) are slightly smaller than that of the filaments in the printed PVA mould (400 µm × 200 µm), due to shrinkage during curing of the PDMS elastomer. A random pore region can be seen in the area between two rows of structured pores (blue dotted lines).

To demonstrate the possibility of controlling the size of the random pores, the previously described PVA mould was filled with smaller salt or sugar crystals, yielding scaffolds shown in **Fig. 7** (using 20-40 µm salt crystals) and **Fig. 8** (using 100-200 µm sugar crystals, here casted with PCL in stead of PDMS).

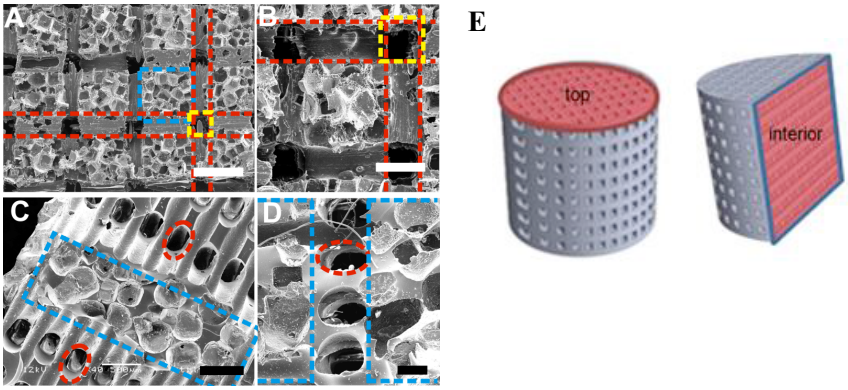

Figure 6. SEM images of fabricated dual-pore PDMS scaffolds (structured pore size 400 µm × 400 µm, distance between structured pores 800 µm; random pore size 300-600 µm): A) top view showing structured pores and an array of random pores; B) magnification of the top view in (A); C) cross-sectional view of structured and random pores; (D) magnification of the top view in (C). (Dashed lines: yellow – structured pores in z-direction; red - structured pores in x or y-direction; blue - random pores area) Scale bars: A) 1mm; B) and C) 500 µm; D) 250 µm. E) Schematic of top view and cross-section view of the interior regions of the scaffolds.

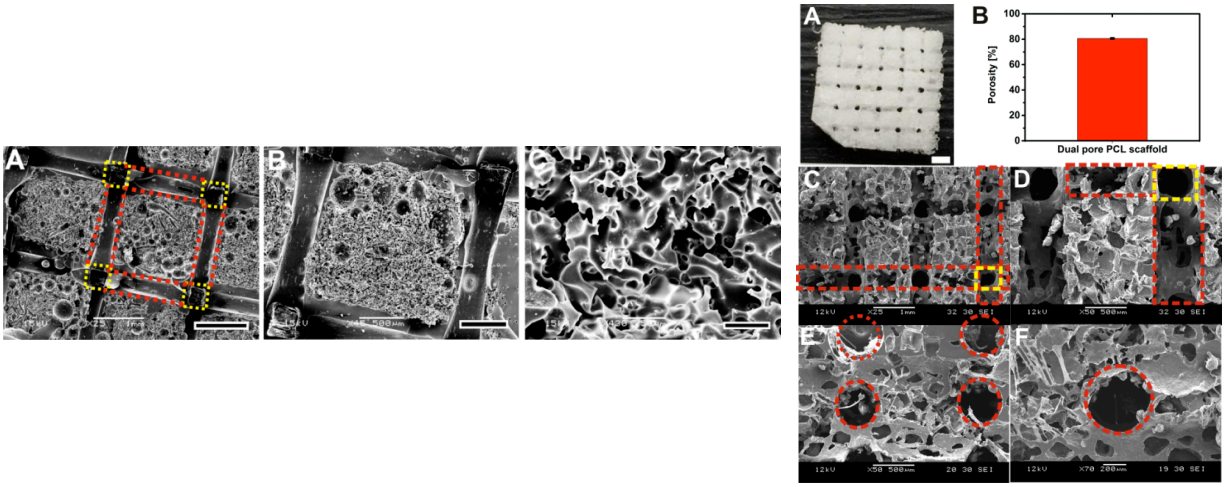

Figure 7 (left): SEM images of dual pore PDMS scaffold with structured pore of dimension 400 µm and random 8 pores of 20-40 µm. Scale bar: (A) 1 mm, (B) 500 µm and (C) 50 µm. **Figure 8 (right):** (A) Photographs of dual pore PCL scaffold casted from combined salt (particle size 100-200 µm) and PVA (40% porous) mould. (B) Calculated porosity of the scaffold. (C) SEM micrographs of 3D PCL scaffold's top view with 400 µm of structured and 100 -300 µm of random pore size. (D) Zoom in of C. (E) Side view from the centre of the PCL dual pore scaffold. (F) Zoom in of E. The scale bare is 1 mm in A and C, 500 µm for D and E and 200 µm for F.

In addition to the woodpile structures shown above we also fabricated hexagonal pore architecture as shown in **Fig. 9**, and the scalability of the process is illustrated in **Fig.10.**

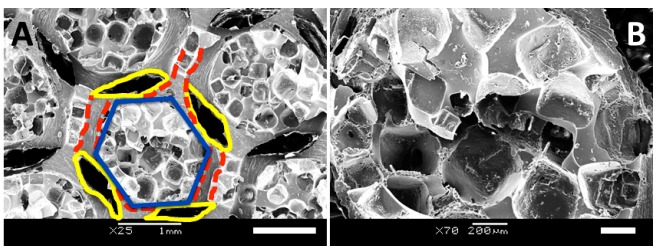

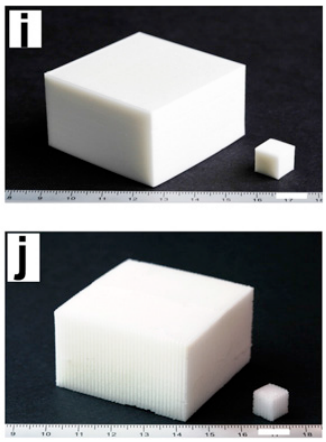

Figure 9 (left): SEM image of hexagonal dual pore scaffolds (A) and zoom in into the random pore region of dual pore scaffold (B) (red: structured pore in x-y direction, yellow: structured pores in z direction and blue: random pore region). **Figure 10 (right):** Scalability of process: Photographs of a large and small PVA mould (I) and resulting PDMS scaffolds (J).

In **Fig. 11** we demonstrate the impregnation of 80% microporous 3D PDMS scaffolds with pHEMA-co-PEGMEA hydrogel using sCO_2, as schematically illustrated in **Fig. 11A**, also showing photographs of disc-shaped scaffolds before (**Fig. 11Ad**) and after (**Fig. 11Ae**) IPN has been introduced. SEM images of the top (**Figs. 11Bab**) and side view (**Figs. 11Bcd**) of fabricated 3D IPN PDMS scaffold show a highly interconnected square profile (average side length 350 um) with elliptical shaped channels (average width 400 µm, height 200 µm), respectively. The channel dimensions in the 3D IPN PDMS scaffold are slightly smaller than the dimension of the base 3D PDMS scaffold due to the swelling of the PDMS when impregnated with hydrogel. 3D filament printing is favourably used to make 3D IPN scaffolds for two reasons: 1) Dimensions and geometries of the pores of the scaffolds are highly tuneable and controllable. 2) Since the pores of the scaffolds are highly structured with interconnected channels they are easy to clean, removing any uncross-linked monomers or cross-linked hydrogels deposits connected around the porous, by simple perfusion with water/buffer.

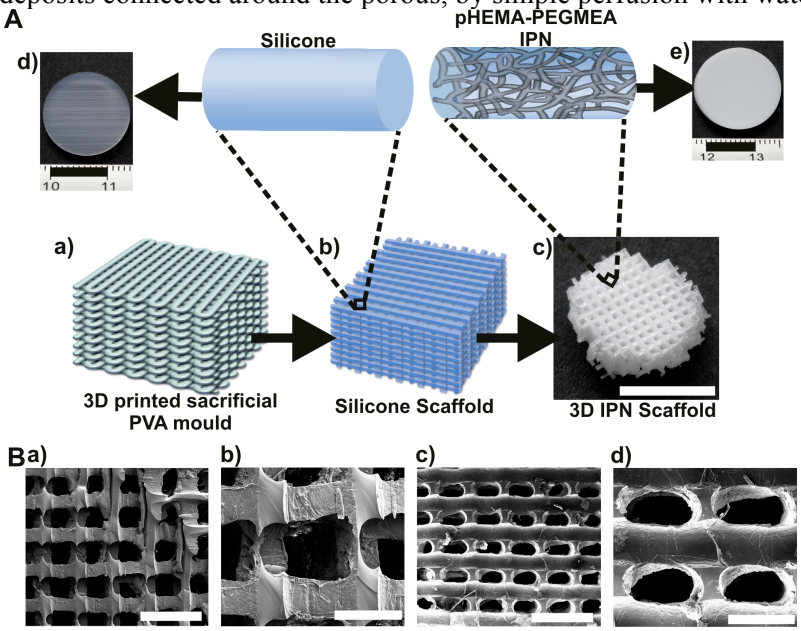

Figure 11. (**A**) Schematic illustration of the process of producing a 3D IPN scaffold, starting from a 3D printed sacrificial water soluble PVA mould (a), via silicone elastomer casting around the PVA mould and its subsequent removal to form a 3D silicone scaffold replica (b), to its subsequent hydrogel impregnation via sCO2, generating an 3D IPN scaffold (optical image) (c). (**B**) SEM images of top (ab) and cross sectional view (cd) of 3D IPN scaffolds. Scale bars: 1 mm for A and C; and 400 µm for B and D.

Apart from silicone elastomer scaffolds, biodgradable scaffolds in gelatin and silk have been developed using the same fabrication strategy as described above. All scaffolds were moreover characterized in terms of their physicochemical characteristics and biocompatibility, and finally applied for growth and maturation of hiPSCs-derived BALs, as will be described in section 4.1.3.3.

4.1.3.2. Human pluripotent stem cell (hiPSC) technology

Summary

Cellartis has had the main responsibility for this activity, some of which has been performed in collaboration with DTU and RUG relevant to WP4 and WP5. The ultimate goal has been the effective production of large amounts of human induced pluripotent stem cell (hiPSCs)-derived hepatocytes in 3D cultures. Culture conditions were thoroughly optimized in several different aspects in order to have

the best possible protocol for maturation of hepatocytes. Collectively, these efforts have produce 3D liver tissues, which were optimized to ensure that the microenvironment aligned as close as possible with that found *in vivo*. State-of-the art maturity and functionality of hiPSC-derived hepatocytes and hepatospheres has been achieved.

S&T results

Cellartis has successfully achieved proof of concept in passaging hiPSCs and scaling up through 3D spheroid culture in a standardized procedure. A summary of the performed studies is presented in **Figures 12-15.**

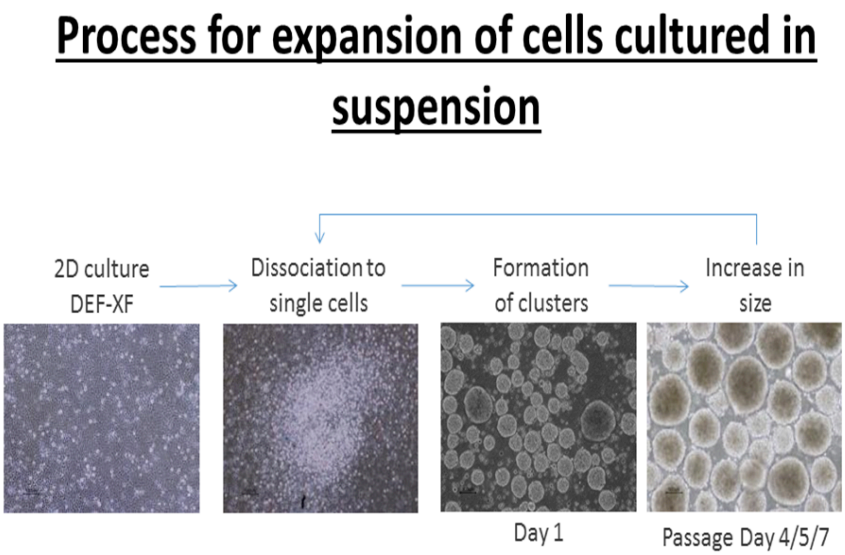

Figure 12. hiPSCs were cultured in conventional 2D culture system (i.e. cells are attached to a coated surface area in flasks). Following expansion in 2D culture, the cells were dissociated into single cells and allowed to form small spheres/clusters in suspension culture. The spheres were then increasing in size over the next 4-7 days followed by a new round of dissociation and reseeding.

The 3D suspension expansion method seemed to keep the cells undifferentiated similar to conventional 2D expansion, but the cell yield was fairly low when cells were only passaged every 7th day (**Fig.13A, left bars**). When the cells instead were passaged in a 4-5-5 day schedule, the cell yield increased dramatically (**Figure 13A, right bars**).

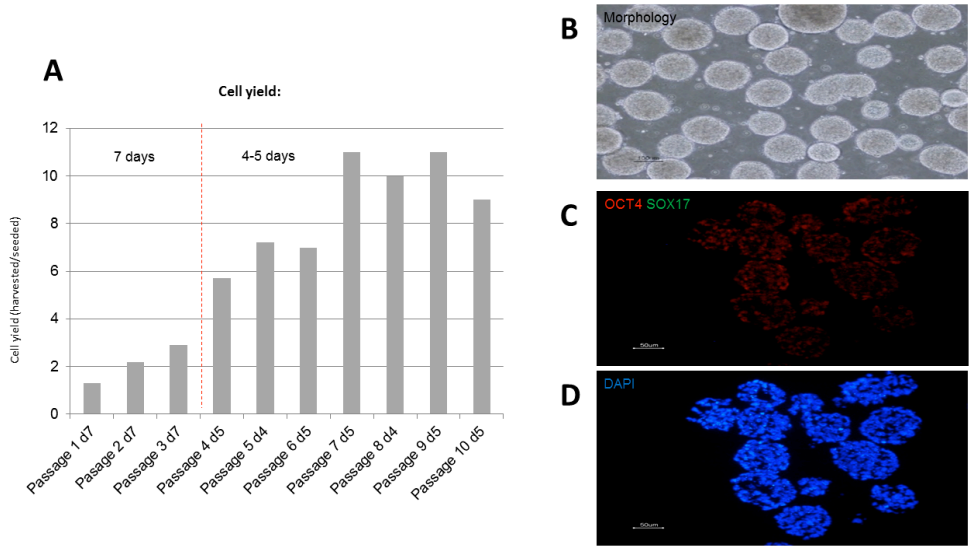

Figure 13. The cell yield is drastically increased when the spheres are passaged in a 4-5-5 day schedule, rather than in a weekly schedule. (**A**) The number of cells at day of harvest was calculated and presented as cell yield at

day of harvest divided by the number of cells seeded at day of passage. (**B-D**) Morphology of the spheres at day of passage: The spheres were fixed and stained for the presence of Oct4 (C, red, a marker for the undifferentiated state) and Sox17 (D, green, an early differentiation marker). Using the optimized culture system, essentially all cells were stained positive for Oct4 and less than 2% stained positive for the presence of Sox17, indicating the still undifferentiated state of the spheres.

At some occasions during the passage schedule, a secondary structure appeared within the spheres. This structure seemed to occur especially at day 5-7, while disappearing when the cells were reseeded. Immunostainings and qPCR-data showed that at later stages of cell growth (i.e. day 5-7) there was an increase in cells stained positive for Sox17, an early differentiation marker for definitive endoderm (**DE**). When the cells were instead passaged every 4-5-5 days, the Sox17 gene was down regulated (**Fig. 14**) and the immunostaining for Sox17 disappeared (data not shown).

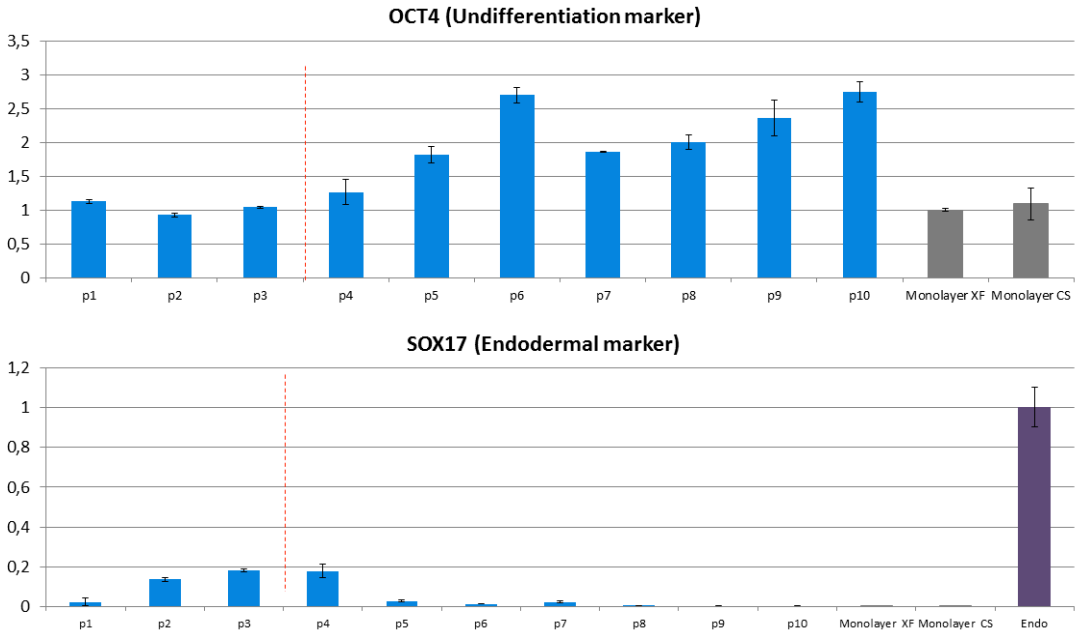

Figure 14. qPCR analysis of hiPSC spheres cultured in suspension with a passage schedule of 7 days for three passages (first three bars), followed by passage in a 4-5-5 day schedule (p4-10). The level of Oct4 increased to a steady level, while the presence of Sox17 expression was decreased to similar levels as for a conventional monolayer culture (see grey bar controls on the right hand, where the expression in monolayer in xeno-free medium is set to 1). Purple bar-control of Sox17 expression in hiPSCs differentiated towards DE.

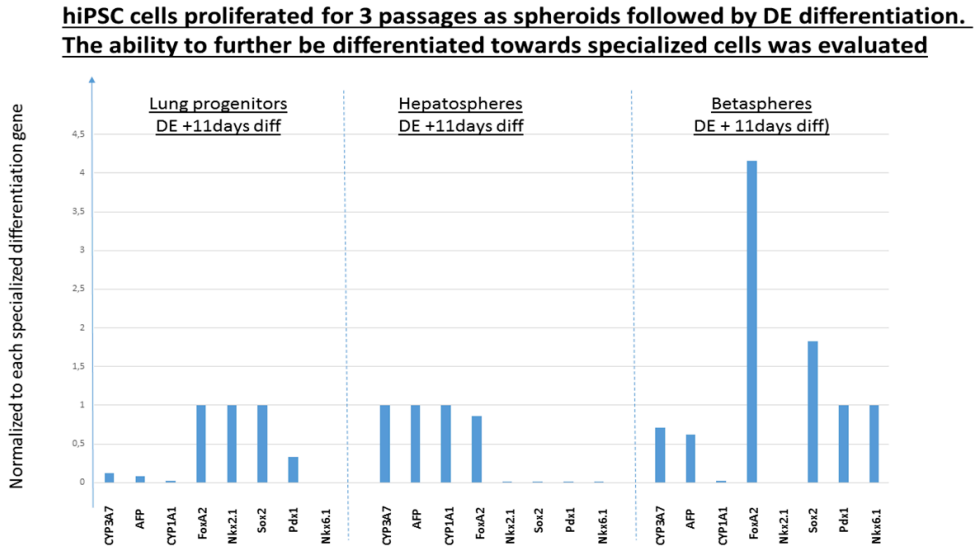

Figure 15. Spheres that had been proliferating for three passages in suspension culture were differentiated towards DE. From the DE stage, the experiment was divided into three groups for further differentiation towards

early lung progenitors, early hepatocytes and early beta cells. The differentiated spheres were harvested 11 days post differentiation towards DE and analyzed by qPCR. Genes that are supposed to be overexpressed in the different specialized cell types were set to 1 and compared to the other two groups. For lung progenitors the genes FoxA2, Nkx2.1 and Sox2 were chosen; for hepatocytes the genes CYP3A7, AFP and CYP1A1 were chosen; and for early beta cells the genes Pdx1 and Nkx6.1 were chosen. Though all genes were expressed in the different specialized cells (since they have the same precursor in the DE stage), it was evident that the different differentiation protocols could drive the cells towards the different stages.

To verify that spheres that had been proliferating for three passages/14 days in suspension culture in the xeno-free medium could differentiate properly, they were differentiated towards the DE stage. Several specialized cell types can further be derived from the DE stage, why the DE spheres capability to differentiate towards lung progenitors (**Fig. 15, left bars**), hepatospheres (**Fig. 15, middle bars**) and beta-cell spheres (**Fig. 15, right bars**) was analysed. The cells were harvested 11 days post the DE stage and analysed by qPCR. The data clearly show that cells in suspension could not only be differentiated to DE, but also further differentiated into lung progenitors, early hepatocytes and beta-cell progenitors.

Increased stability and maturation of frozen DE cells in 2D culture

We noticed that frozen hepatocytes only survived well for 11-14 days post thawing. Since it was essential that the 3D BAL bioreactors could be run over extended periods, we studied whether DE cells would survive better. It turned out that cell cultures derived from frozen batches of DE cells had a much longer survival life span, for which we only tested until day 42 with some very interesting results, described in **Figs.16-19.**

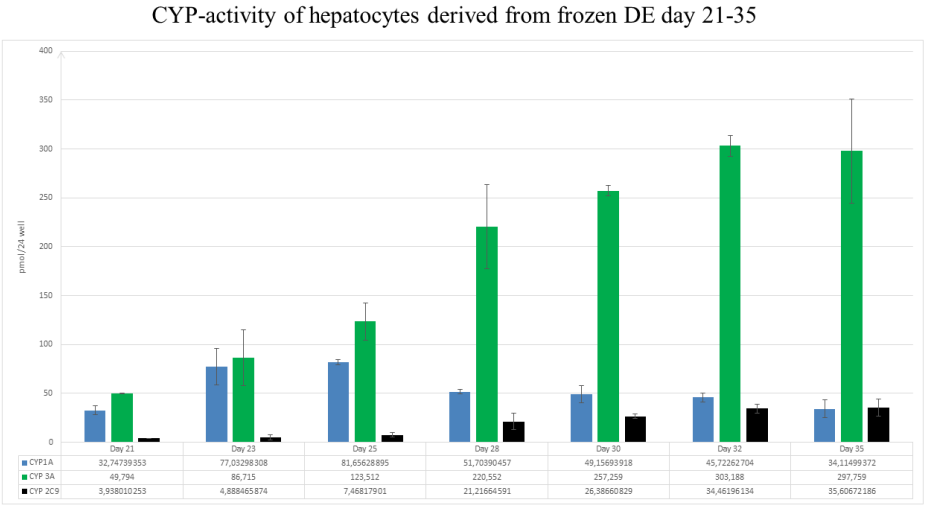

Figure 16. CYP activity of hepatocytes derived from frozen DE cells, measured on day 21, 23, 25, 28, 30, 32 and 35 of maturation (i.e. day 14 – 28 post thaw the DE cells). The CYP activities of CYP3A and CYP2C9 increases over time, and the cells could easily be used between days 21-35 for hepatocyte measurements. Although the CYP1A activity seems to drop slightly over time we believe this is due to the fact that the method cannot distinguish between CYP1A1 and CYP1A2. The expression of CYP1A1 is decreasing over time (data not shown), while the expression of the liver specific CYP1A2 increases (see also **Fig. 19**).

A prolonged culture of the "maturing DE cells" beyond day 32 seemed to allow the cells to mature more over time. Interestingly we could also see a fascinating phenomenon in the culture when the cells were immunostained for the presence of albumin and CYP3A4 (**Fig. 17**). On day 21 post-thaw (day 28 of maturation), the CYP3A staining was quite diffuse with the protein present in many of the cells, while only a fraction of cells contained albumin (**Fig. 17, right images**). However, nine days later (day 30) the morphology and pattern had changed dramatically and one could see "hepatic zonation", normally seen in human liver slices (i.e., cells in a liver either express albumin, which is connected to certain functions, while other cells only express CYPs with yet another function). Interestingly this could now be mimicked in a dish, and further indicates that the cells mature continuously. This is potentially very important for the use and functionality of the maturing DE cells in BAL reactors.

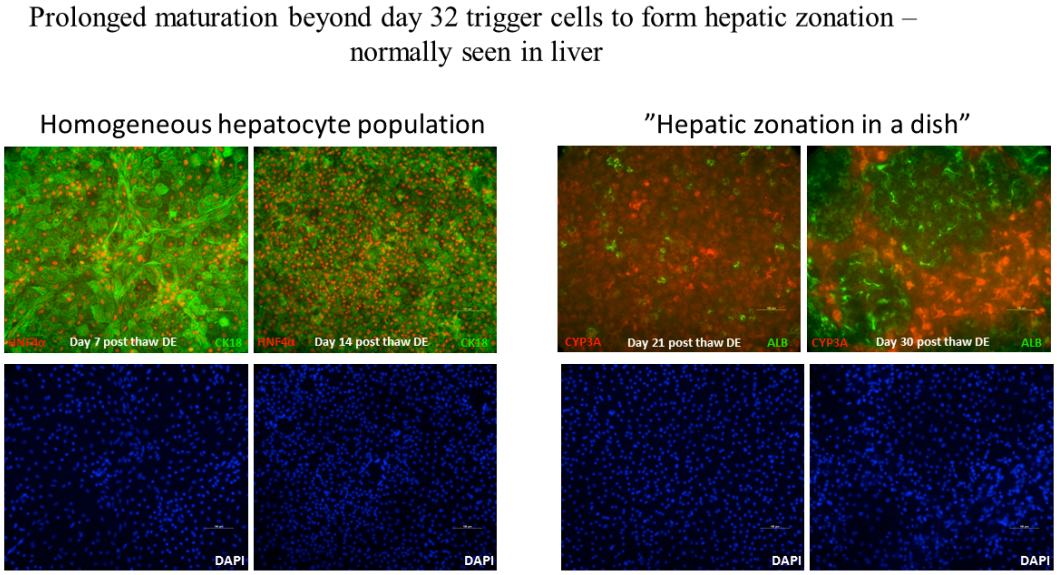

Figure 17. Maturation of the DE cells over time. The left images stained on day 7 and 14 post thaw were stained with HNF4a (red) and CK18 (green) and show that essentially all cells do express those genes and indicate the purity of the established cell culture protocol. At later stages, more adult genes start to be expressed, here visualized by staining of albumin (green) and CYP3A4 (red) shown in the right hand images. At this later stage, the cells clearly show a hepatic zonation *"in vitro"*, i.e., cells either expresses albumin or CYPs and are clearly regrouped in different "zones".

The extended life span of DE cells over frozen hepatocyte cells, as indicated in **Figs. 16-17**, triggered us to investigate whether the cells could survive for yet a bit longer, which would be important for the BAL bioreactor experiments. Cells were therefore matured until day 42 (i.e. day 35 post thaw of the DE cells), and analysed by qPCR (**Fig. 18**) and by CYP activity measurements (**Fig. 19**).

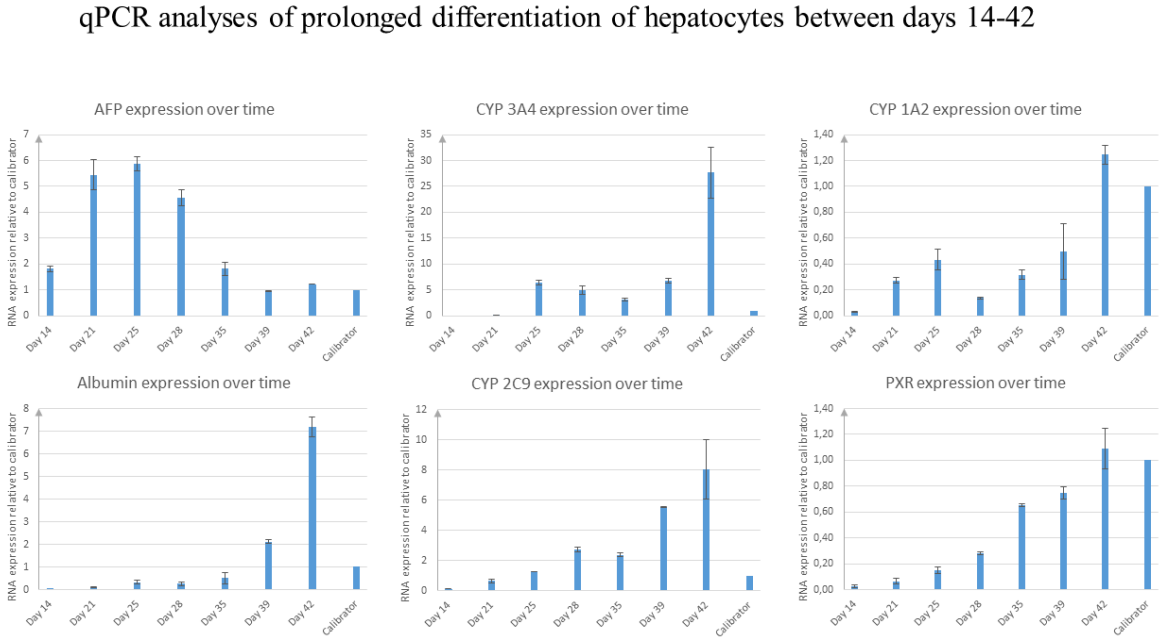

Figure 18. DE maturation towards hepatocytes extended until day 42 (i.e. day 35 post thaw of DE cells). AFP decreased as expected while the mature Albumin expression increased over time, with a dramatically increased expression on day 42. The same interesting pattern could be seen for several other mature genes, such as CYP3A4 (upper middle graph), CYP1A2 (upper right graph), CYP2C9 (lower middle graph) and PXR (lower right graph).

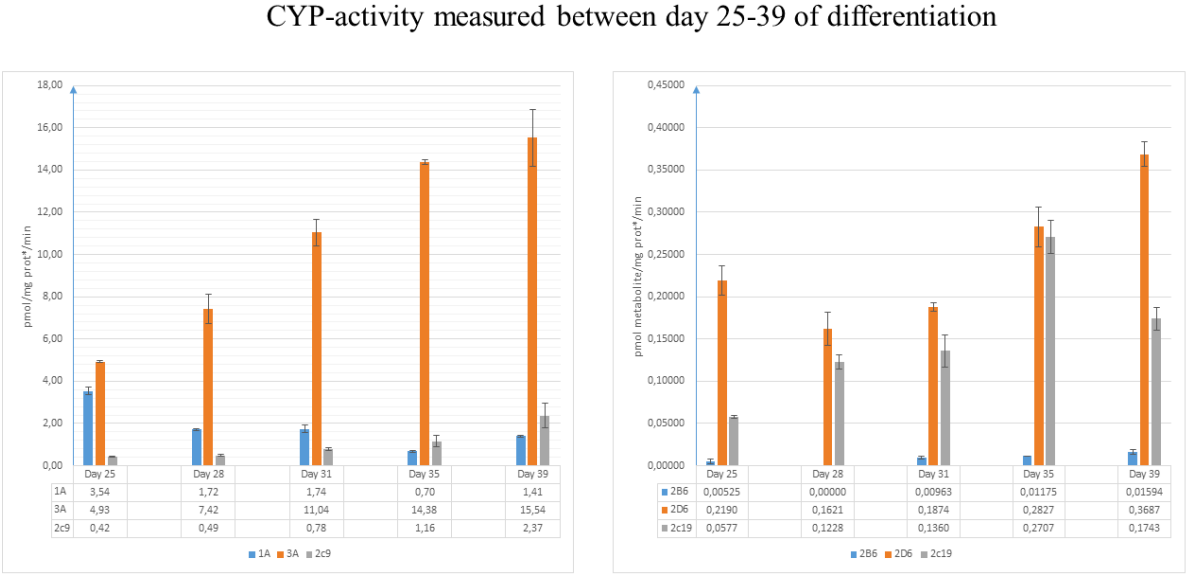

Figure 19. DE maturation towards hepatocytes extended until day 39 (i.e. day 32 post thaw of DE cells). Essentially all CYP activities measured increased over time, with the lower CYP1A activity discussed in **Fig. 16**. Even the lowly expressed CYP 2B6 seems to increase slightly.

3D suspension cultures of hepatospeheres

For future aspects of scale up of hepatocytes it is important to expand stem cells in suspension cultures. Cellartis chose to focus on 3D suspension cultures (**Figs. 13-15**), which made it necessary to be able to differentiate the cell suspension towards the desired specialized cell type. Cellartis thus further developed the "hepatosphere" differentiation protocol, with the aim to: 1) Stabilize the protocol, 2) prolong the maturation stage since initially the hepatospheres gradually degrade over time, and 3) freeze/thaw the hepatospheres.

Hepatospheres seems to mature in a way that cells are inducible when treated with rifampicin, phenobarbital or omeprazole already quite early during maturation (**Fig. 20**). The stability of these experiments need to be further developed, however, this proof-of-concept is of importance since it indicates that the maturation protocol together with the 3D concept indeed can mature the functionality of the hepatocytes, which is hard to achieve in conventional 2D cultures.

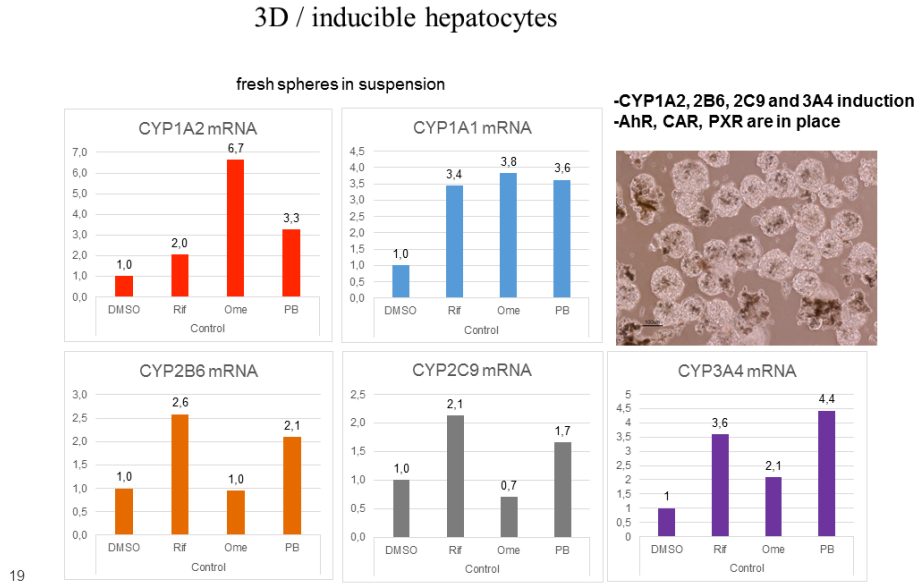

19

Figure 2.20. CYP induction study of spheres in suspension matured towards hepatocytes. Although the induction is still quite moderate it indicates that the maturation and functionality of hepatocytes in 3D suspension format seem to go faster (the spheres are differentiated for 25 days in total, compared to 37 days in **Figures 2.17-2.18**). The functionality of hepatocytes in a liver is highly dependent on the polarity of cells. Speculatively the sphere format can allow the cells to possibly polarize in a different fashion compared to conventional 2D cultures.

4.1.3.3. Sensor and bioassay technology

Summary

Luxcel has had the main responsibility for this activity and has together with DTU and RUG in joint efforts developed a panel of sensor tools and bioassays for operation in conjunction with the BAL system on macro-, micro- and nanoscale, in-line and off-line. Some of these systems were successfully integrated in the BAL support system and tested for their suitability and analytical performance. A number of different options of sensors, measurement formats and bioassays provide the users high flexibility and ability to solve important monitoring tasks during BAL development and optimisation, growth of artificial liver tissue and its operation as BAL. These analytical tools enable implementation of feedback control and optimal operation of the BAL system, and comprehensive assessment of BAL tissue function.

S&T results

Efficient operation of a perfusion-based BAL system requires precise control and optimisation of their key physical, chemical and physiological parameters. Optimal growth and differentiation of hiPSC and preparation of BAL tissue require for instance monitoring of O_2 levels, which is an indicator of optimal flow and mass exchange conditions, uniform tissue growth and functioning inside the BAL system. Precision-cut liver slices used for tissue function and drug toxicity testing also require control of dissolved O_2. To implement this, the team has developed and deployed a range of advanced optochemical and electrochemical (O_2, pH and impedimetric) sensors, and metabolic- and functional assays for liver tissue.

Optical O2 and pH probes
Luxcel has applied the phosphorescence quenching method, which operates with cell-permeable probes and solid-state sensors, to control O_2 levels in BAL and liver slice systems in a non-invasive, contactless manner. Control of tissue pH and acidification rate is also realised in a similar manner using a luminescence based pH sensitive probe. Different types of phosphorescence based O_2 sensor systems and fluorescence based pH sensors, include:

1. Solid-state sensor coatings (GreenLight™ chemistry with NIR spectral characteristics), which can be applied on the inner wall of BAL device or outer surface of the scaffold material (prior to their assembly), and then interrogated from outside of the biochip with a handheld phosphorescent detector (Optech, Mocon-Luxcel), which gives quantitative readout of O_2 concentration in this particular area of the device (2-5 mm spots or bigger zones). The sensors can be incorporated at the entrance and exit ports of the device, to measure
2. Cell-impermeable extracellular O_2 probe MitoXpress™ –Xtra with visible spectral characteristics, which is introduced in perfusion medium to allow O_2 measurements in tissue biochips on a commercial fluorescent plate reader. In this case, O_2 can be probed in different locations of the whole chip (area 3-5 mm^2, spatial resolution ~1 mm). The limitations are that the biochip must be placed in the microplate compartment of the reader (usually not a problem for the biochip itself, but for the fluidic part (tubing and ancillary) and that significant quantities of the probe are wasted.
3. Cell-permeable intracellular O_2 probe NanO2 having visible spectral characteristics, which are added to the medium only when the cells/tissue are loaded. These probes penetrate the cells and remain there for prolonged periods of time. They allow point measurements of local O_2 levels in

tissue sample or in different parts of the biochip system of scaffold structure, which can be realised on a commercial time-resolved fluorescence plate reader, in a format similar to point 2 above.

4. Extracellular pH sensitive probe pH-Xtra, which can also be measured on a time-resolved fluorescent reader in lifetime-based sensing mode, and which is multiplexable with MItoXpress-Xtra O_2 probe without any cross-sensitivity.

Spectral characteristics of the O_2-sensitive materials are shown in **Fig. 21.** Operational performance of the sensor systems was evaluated in several physiological studies with different cell and tissue models. **Fig. 22** shows a commercial biochip, designed for live cell imaging (panel **A**), in which O_2 sensors were incorporated. Using the O_2 probes, oxygenation of cells seeded in the biochip micro-chambers was measured, revealing that high cell density makes the system anoxic under static conditions (panel **B**). On the other hand, perfusion of the micro-chambers with fresh media (manually with a pipette) transiently increases the O_2 levels. This also allows measurement of oxygen consumption rate (OCR) on a fluorescent plate reader (panel **C**).

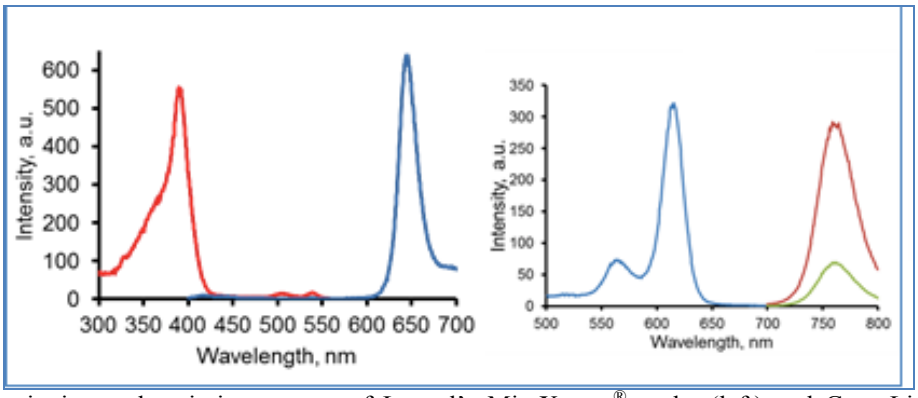

Figure 21. Excitation and emission spectra of Luxcel's MitoXpress® probe (left) and GreenLight™ sensors (right): Phosphorescent signals in completely deoxygenate (red) and air-saturated (green, 210 mM O_2) conditions are shown on the right panel.

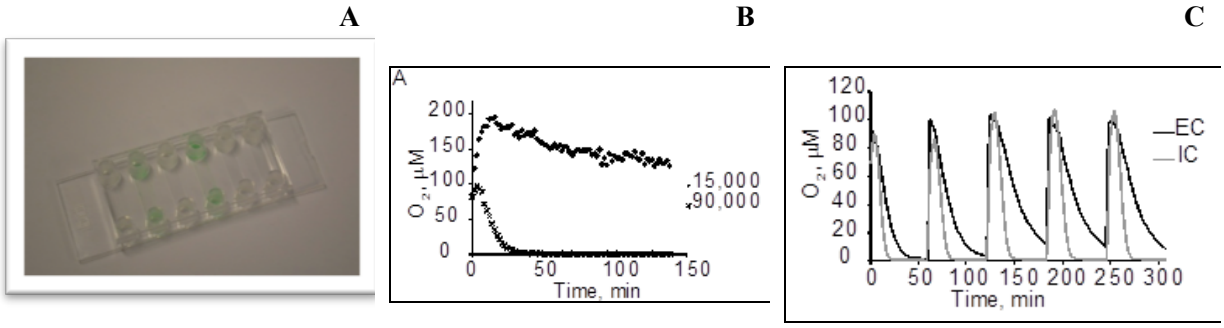

Figure 22. Measurement of cell oxygenation and OCR in commercial multi-channel biochips Ibidi (Germany). A: photograph of a biochip with GreenLight sensor deposited at the entrance and exit channels. B: Oxygenation profiles of MEF cells seeded in the biochip at different density and maintained under static conditions (measured with MitoXpress probe). C: OCR measurements of MEF cells in Ibidi chips by repetitive perfusion of samples with medium, performed with both intracellular and extracellular O_2 probes.

The OCR assays based on Luxcel O_2 probes were applied to Cellartis liver stem cells (hiPS-HEP™), where they showed good analytical performance, sensitivity in detecting minor changes in OCR (Z-factor = 0.69), general flexibility and robustness (**Fig. 23**). In these studies, the O_2 monitoring systems were also tested and validated with several other cells including HepG2, HepRG, PC12, HCT116, and primary cells (cortical neurons and CGNs).

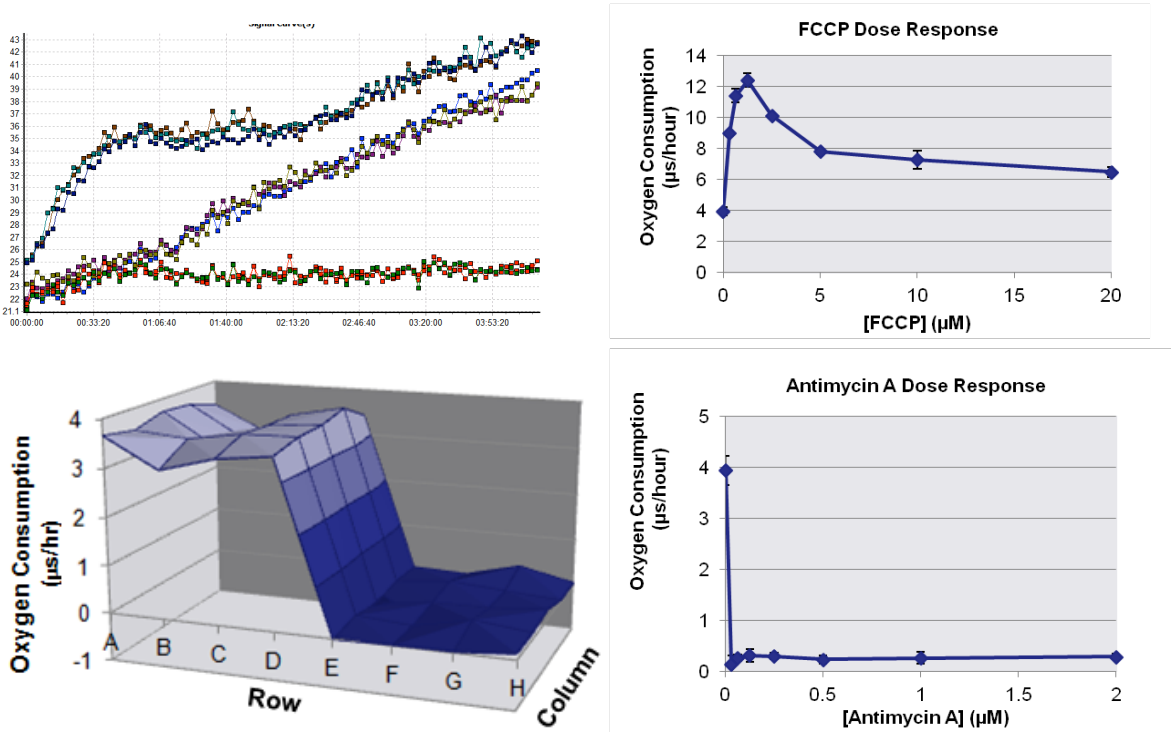

Figure 23. OCR measurements with adherent liver stem cells (hiPS-HEP™, Cellectis) and Luxcel O_2 probes, performed in standard 96-well plates on a time-resolved fluorescence plate reader BMG

Following the successful development, testing and optimization of the new sensor materials, their deposition or application procedures and production of first prototype biochips with built-in O_2 sensors, Luxcel together with the other partners started to integrate these analytical tools in the BAL systems. The solid-state O2 sensitive coatings were incorporated in the perfusion system (**Fig. 24**) and allowed control of oxygenation of incoming and outgoing medium and assessment of oxygen consumption rate (OCR) with a simple and affordable instrument Optech™ (Mocon).

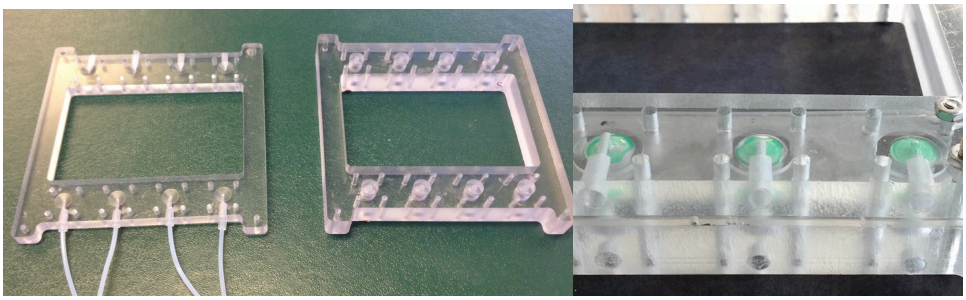

Figure 24. The components of the BAL bioreactor system and O_2 sensors incorporated in them.

Luxcel has moreover developed several families of cell-penetrating phosphorescent O2-sensitive probes – polymeric nanoparticles and small molecule structures. A new family of O2 probes based on conjugated polymers co-polymerized with a phosphorescent dye and prepared as nanoparticle formulation (**Fig. 25**) was developed. The new probe design provides enhanced (~10-fold) brightness and stability, more uniform cell/tissue staining, better penetration into tissue. It also allows tuning of the nanoparticle surface charge (cationic, anionic or zwitterionic), cell specificity and permeation mechanism, and production of several spectral variants with UV/Vis excitation and red/NIR emission.

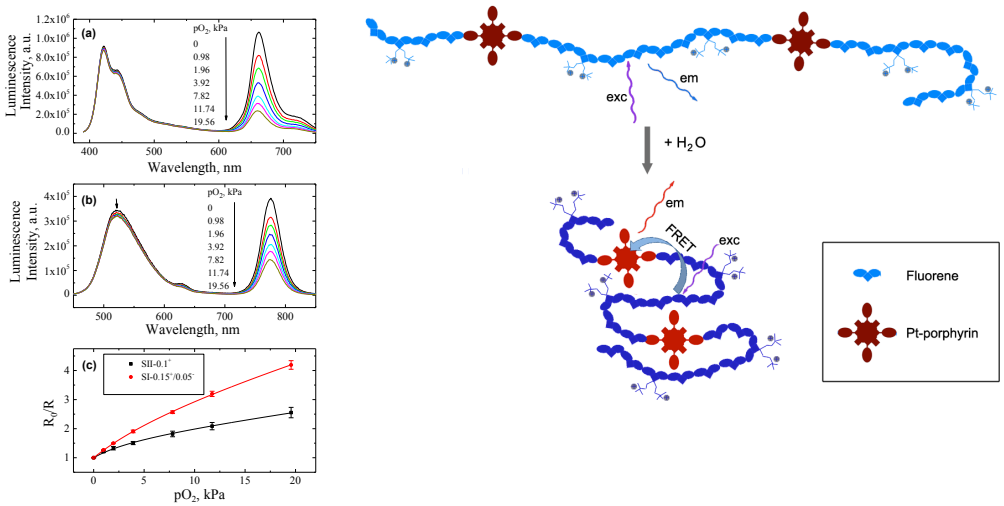

Figure 25. Structure of the new nanoparticle based O2 probe based on conjugated polymers (above) and its spectral and O2 sensing characteristics (left panel).

The new O_2 imaging probes were evaluated in a number of different models of mammalian tissue and physiological studies, using the confocal Phosphorescence Lifetime Imaging Microscopy (PLIM) system installed in Luxcel's lab. In particular, high-resolution O2 imaging studies were carried out with the following cell and tissue models: Cellartis hiPSC, HepG2, HepRG, HCT116 cells, MEF, A549, primary neurons, neurospheres, cancer cell spheroids (HCT116). Moreover, several different types of mammalian tissue were used in complex physiological studies with O2 imaging: brain tissue slices from embryonic rats, mouse colon, bladder tissue, pig's eye cornea. Representative images are shown in **Fig. 26**.

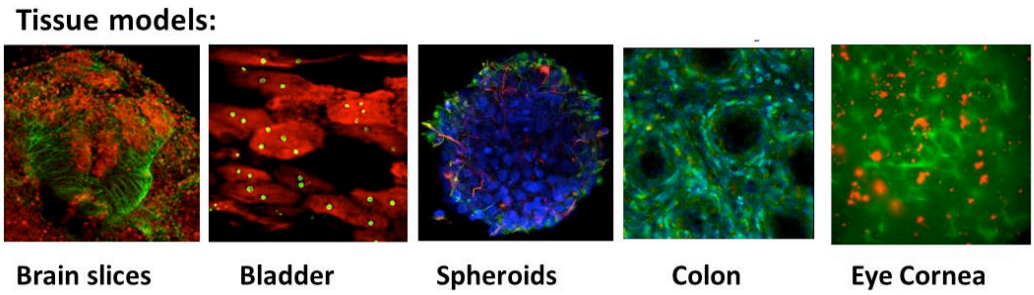

Figure 26. Images of the different tissue models stained with the phosphorescent O_2 sensing probes.

Impedance based sensing tools

Electrical impedance spectroscopy (EIS) is a technique to describe material properties as resistance to electrical current flow and their ability to store electrical charge, which mainly depends on tissue composition (i.e. cellular size and density, cellular spacing and the constituents of the extracellular matrix) in biological materials. This technique has been demonstrated as a powerful tool for the real-time study of complex biological systems both in vivo and in vitro, by establishing a physical correlation between the electrical measurement and the biochemical phenomena occurring within the sample in a non-destructive way.

In order to maximize the biophysical information gathered through EIS measurements, it's crucial to tailor parameters like electrode number and geometry, orientation and spacing. To enable a comparison, three different measurement configurations (prototypes) were evaluated for the generated current density and sensitivity field. The different impedance based systems developed by DTU are listed below:

1. Prototype 1: Plate-based 4-electrode array platform for monitoring cells growth in static 3D cultures (achieved at month 6). The platform allows combining impedimetric monitoring with 2T

and 3T sensing configurations to build different and complementary multiplexing-like modes that enable collecting spatial distributed information of the biochemical events occurring inside the culture chamber. This approach constitutes a first attempt of generating a flexible EIS based method for monitoring 3D cell cultures and hence bridges the gap between conventional EIS and more advanced electrical impedance tomography. This work is described in detail in delivery report D.3.3

2. Prototype 2: Needle based 4-electrode array platform for tomography-like analysis in static 3D cultures (achieved at month 12). The platform allows collecting spatial distributed information during the process of 3D cell culturing by combining four different 4T-sensing configurations for a tomography-like analysis.
3. Prototype 3: Needle based 8-electrode array for electrochemical impedance tomography (EIT). To potentially image cells and tissues in 3D, see **Fig. 27**.
4. Perfusion based BAL support cell-on-a-chip system with embedded sensors for electrochemical impedance spectroscopy (EIS) analysis, see system design in **Fig. 28** and impedance monitoring of the growth of the BAL in **Fig. 32**, in **section 4.1.3.4**.

Fig. 27 shows our latest system that has enabled us to make preliminary impedance tomography images of tissue constructs

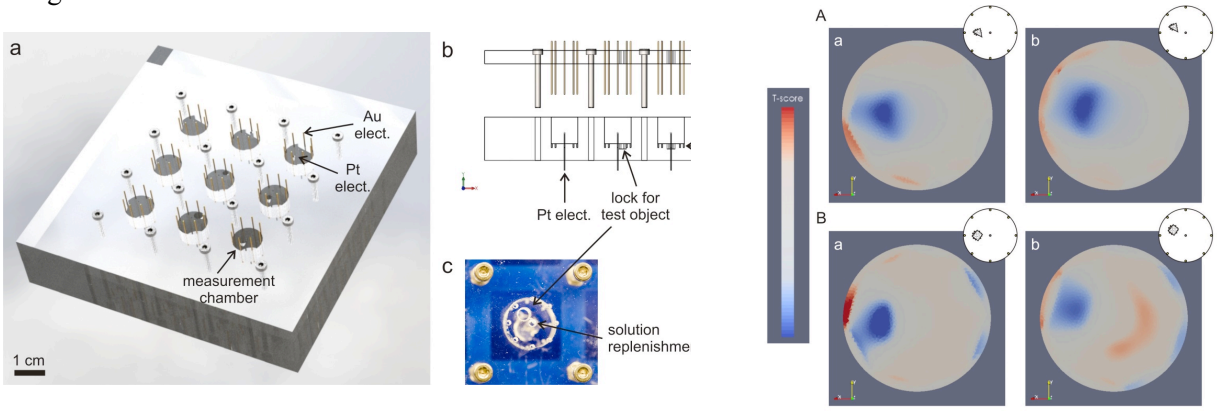

Figure 27. **Left:** (a) The measurement chamber array used for impedance tomography. Eight Au plated electrodes were placed at the periphery of each chamber. When present, the Pt electrode was placed at the centre of the chamber through the bottom plate (8+1 electrodes). (b) Schematic (side view) showing the Pt electrode, the circular slits for positioning the Au electrodes and micromilled depressions at the bottom of the chamber to keep the Au electrodes and the test object in position. (c) Photo of a measurement chamber. The lid had an opening to lock the test object in position and a smaller opening for solution replenishment. **Right:** Image reconstruction in (Aa and Ba) time based EIT and (Ab and Bb) frequency based EIT for an irregular triangular and square shaped potato object placed in the measurement chamber filled with electrolyte. The real position is shown in the inserts at the top right. Images for a (A) triangular object and (B) square shaped object in two alternative positions: 2.5 mm radial centre-to-centre distance between the phantom and the chamber, (a) angle of 135° and (b) angle of 112.5°. The colour scale is in arbitrary units (from -1 in blue, to +1 in red) representing the T-score.

4.1.3.4. Technology Integration and BAL development

Summary

This activity has been the responsibility of DTU Nanotech, working in close collaboration with other partners, especially with Cellartis and RUG in relation to growth of the BAL under perfusion control (DTU & Cellartis) and its further analysis and assessment (DTU & RUG). The activity has involved the fabrication and integration of perfusion based BAL-on-a-Chip and Liver-on-a-Chip systems and BAL support systems incorporating pumps, sample reservoirs, bioreactors, 3D scaffolds and different types of sensors. The systems were successfully tested for their ability for long-term growth and differentiation of hiPCS-derived DE cells and hepatospheres into functional 3D BALs.

S&T results

Two versions of a perfusion bioreactor array platform – **the BAL support system** - were developed. The first version (**Fig. 28**) is a 16-bioreactor array intended for medium throughput optimization experiments of cell culture conditions. The second version (**Fig. 28Ab**) is an 8-biorector array with integrated vertical needle electrodes for electrical impedance spectroscopy (EIS) analysis of cell proliferation over time. The main components of the BAL support system include: (1) an exchangeable bioreactor array chip (BAL-on-a-Chip) for performing cell culture in a 3D environment, and (2) a mother board containing all necessary components such as vials and vial trays for storage of culture medium and waste and peristaltic pumps and motors for perfusion of cell culture medium. **Fig. 28Ae** schematically illustrates the perfusion culture system and fluidic/air circuit, which is the same for both platforms. Four (**Fig. 28Aa**) or two 8-channel micropumps generate pulsatile flow and are controlled by motors and controllers from the Lego Mindstorm kit (Lego, Billund, Denmark). This allows culturing of cells at up to four different flow rates in a single experiment. The pumps allow flow rates from sub-µL·min^{-1} and up to approximately 90 µL·min^{-1}. The fluidic circuit is formed by the pumps, bioreactor array and medium storage vials that are connected using PTFE tubing with inner diameter of 0.8 mm. Inlet and outlet vials are coupled with PTFE tubing and supplied with air supplemented with 5 % CO_2 through a sterile 0.22 µm filter. All components are mounted onto a base platform for portability and easy handling. The entire system is placed in conventional cell culture incubators during the experiments.

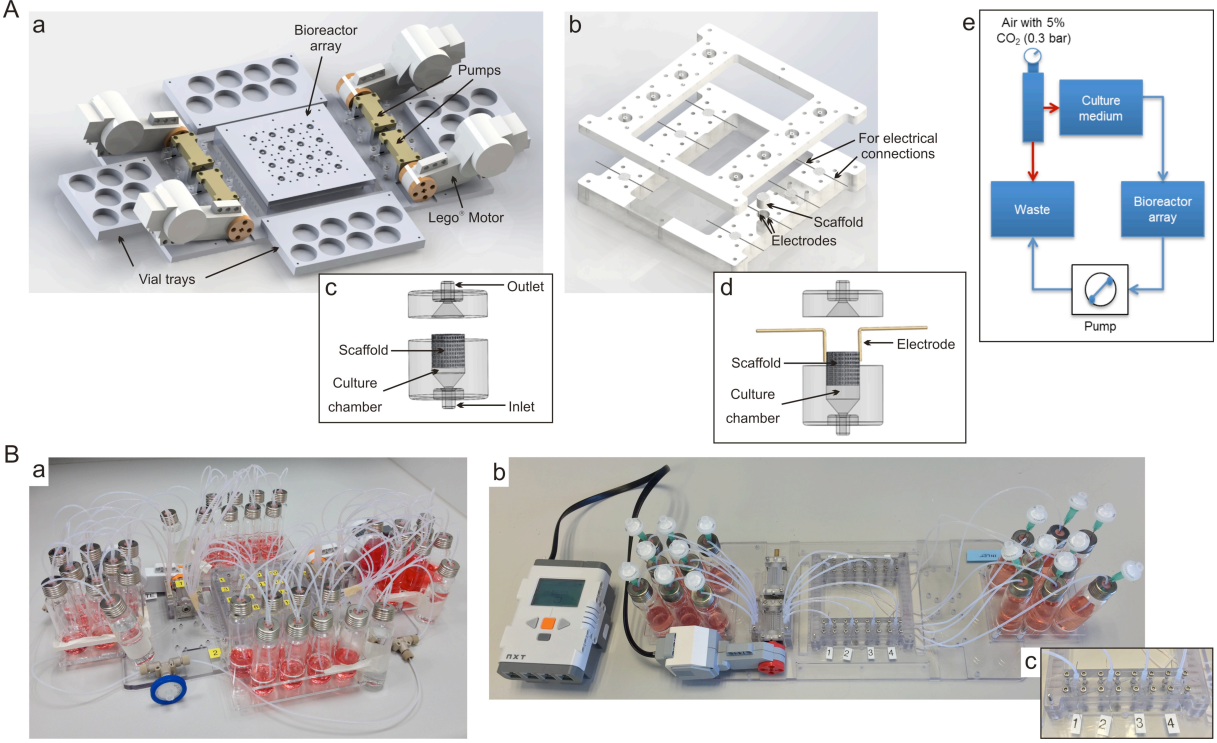

Figure 28. (A) Schematic design of a motherboard having an exchangeable bioreactor array with (a) 16 bioreactors (4 × 4 array) inserted and (b) an 8 bioreactor array (4 × 2 array) with integrated needle electrodes for electrical impedance monitoring of cell proliferation over time. Schematic of the bioreactors in the (c) 4 × 4 array and (d) 4 × 2 array. (e) Schematic of fluidic circuit (blue arrows) and pressure circuit (red arrows). – (B) Assembled perfusion array platform with (a) 16 and (b) 8 bioreactors, the latter with (c) two integrated vertical needle electrodes in each bioreactor.

The bioreactor array allows cell culture in cylindrical 3D scaffolds having diameter of 6 mm and height of 5 mm (**Fig. 28Ac** and **28Ad**). Each bioreactor consists of an inlet port (at the bottom), a cylindrical chamber for housing a 3D scaffold and an outlet port (at the top). Silicone tubes (inner diameter of 1.8 mm and height of 10 mm) are press fitted to the ports of the bioreactor (inner and outer diameter of 1 mm of 2 mm, respectively) and serve as connectors between the bioreactor and the rest

of the perfusion network. The bioreactor units are implemented into the arrays to enable parallelized analysis. **Fig. 28Ac** and **28Ad** show the schematic of a single bioreactor in the case of the 16- and 8-bioreactor array, respectively. For the impedance measurements, two platinum (Pt) needle electrodes (diameter of 0.4 mm and height of 5 mm) were vertically placed at the opposite sidewalls of each bioreactor (**Fig. 28Ad**). Moreover, in the 8-biorector array an opening was introduced between the two rows of bioreactors to allow electrical connections to the electrodes via crocodile clips (**Fig. 28Ab**)

When performing 3D perfusion cultures the main parameters taken into consideration are:

- The optimal flow rate, which is a balance between causing shear forces on the cells and ensure sufficient supply of oxygen and nutrients as well as removal of cellular waste products. Another issue is related to cell secreted signalling factors, as high flow rates will affect autocrine/paracrine signalling, that might be necessary for cell viability and differentiation.
- Scaffold design, which will influence the flow profile through the tissue and thereby the applied shear stress and nutrient supply.
- Medium composition, especially the concentration of the differentiation cocktail of signalling factors. During flow, the concentration of added factors is constant while at static conditions in a batch culture the concentration decreases between each change of medium. Thus, a lower concentration than the one optimized for static batch cultures might be better at flow conditions.

These are factors that all have been taken into consideration when developing and performed many of the experiments described in the following tasks.

Distribution, attachment and differentiated morphology of hiPSC-derived DE cells
The distribution, attachment and differentiated cell morphology of hiPSCs-derived DE cells were evaluated by imaging of the middle of a cross-sectioned scaffold after 22 days of culture at 1 µL/min flow rate in differentiation medium in the 16-bioreactor array system in **Fig. 28Ba**.

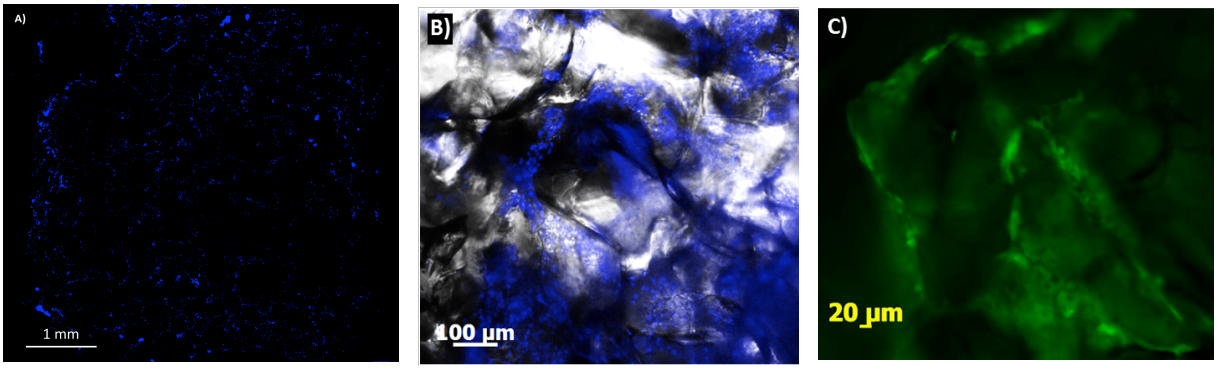

Figure 29. Microscopy imaging of hiPSC-derived DE cells cultured and hepatically differentiated inside a porous 3D scaffold at perfusion conditions: Image at day 22 after cell seeding of the middle of a cross-sectioned scaffold. A) Scan of entire cross-sectioned scaffold showing cell distribution. Höchst stained cell nuclei in blue color. B) Close-up view of cell distribution with Höchst stained cell nuclei. The fluorescence image is merged with a phase contrast image of the scaffold. C) Calcein-AM live-stained cells in green.

As shown in **Fig. 29A** and **B** of Höchst stained cell nuclei, the cells are uniformly distributed throughout the entire scaffold, but residing in populations in the cavities of the porous scaffold. A close-up image of live-stained cells in **Fig. 29C** displays proper cell attachment and morphology. Moreover, in **Fig. 30**, images of DE cells, differentiated on PDMS and on a polystyrene reference show that DE cells obtain identical morphology on PDMS.

The effect of scaffold design- and flow rate on hepatic differentiation, metabolic activity and function of the BAL was further investigated, but is described in detail section 4.1.3.5.

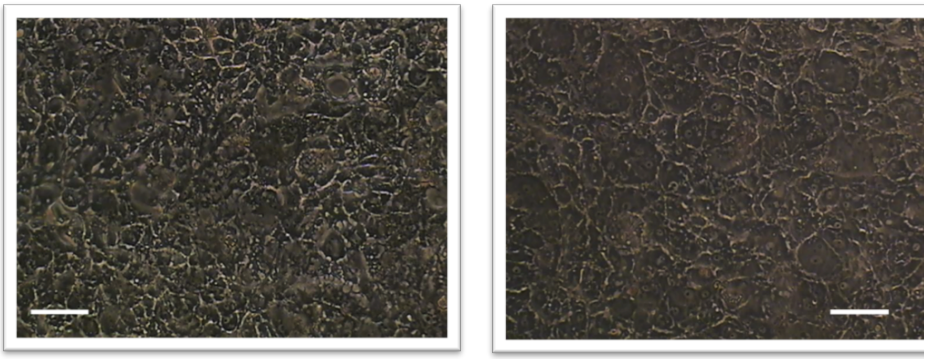

Figure 30. Optical images of the morphology of DE cells differentiated in 2D PDMS sheets (using Cellartis ECM coating), compared to a 2D static reference culture on polystyrene (using Cellartis ECM coating): Both images represent differentiated cells at day 19 of differentiation after the DE stage. **Left:** Reference culture**. Right**: PDMS sheets. Scale bars=60 um.

Culture of hiPSC-derived hepatospheres in the BAL

Experiments were conducted with GFP tagged pre-differentiated hepatospheres fresh from Cellartis, which were loaded into BALs having scaffolds with either large or small pores, using gravity or centrifugation at 50 x g for 10, 20 and 40 seconds. The scaffold were cut in two and visualised by microscopy to investigate what porosity of the scaffold was optimal for loading the spheroids.

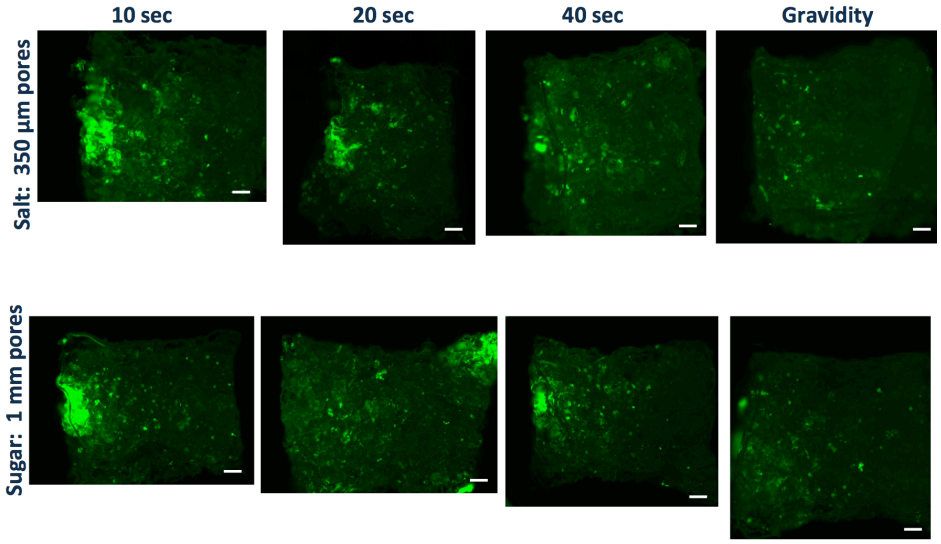

Figure 31. Scan over entire scaffold to detect GFP labelled hepatospheres. The BAL scaffolds were cut lengthwise in the flow direction and scanned in a fluorescent microscope. Scale bar: 500 µm. The loading direction is from left to right in each image.

Microscopic inspection show that the hepatosphere could be trapped inside any of the two random PDMS scaffolds (**Fig. 31**), and moreover that they could be cultured and matured in the BAL support system during 15 days. Gene expression- and albumin secretion analysis moreover indicated that populating the scaffolds with hiPSC-derived spheroids, produced in suspension culture, followed by perfusion culture of these in the BAL support system may be a more viable and cost efficient way to produce a final BAL.

Impedance monitoring of cell growth in BAL support system

Using the BAL support system in **Fig. 28Bb**, impedance monitoring of cell growth in the porous 3D scaffolds over a 19-day period was performed after loading of cells using a suspension with density of 2 × 10^6 Heg2 cells in 30 µL. **Fig. 32A** shows the measured impedance magnitude at 10 kHz over time. A drop in impedance was observed during the first three days of culture, which was a surprise. However, we reasoned that it could likely correspond to a loss of non-adherent cells when perfusion was turned on, moreover calculations on the theoretically predicted number of cells that could be housed in the scaffolds was determined to be much lower than the number of cells that were loaded/seeded (see task

4.3 for calculations). After an initial decrease of impedance during the first three days, it started to continuously increase over time. To understand these results, the cell number was determined based on the dsDNA content of cells in the scaffolds, using the PicoGreen assay. In fact the number of cells at the end of the 19 days cell culture period was found to be lower than the number of cells seeded into the scaffolds at the start of the experiment. This is also indicated by the impedance spectra of **Fig. 32A**, showing a lower impedance magnitude at the end of the culture period compared with the magnitude at the beginning. **Fig. 32B** shows correlation between the measured impedance at day 19 (evaluated at 10 kHz) and the determined dsDNA quantity (day 19) in the different scaffolds. A parallel experiment was performed where scaffolds were loaded with 2×10^6 cells and then perfused with medium in the bioreactors. After 24 hours, we found that only $0.9 (\pm 0.2) \times 10^6$ cells (mean ± SD, n = 4) remained in the scaffolds, confirming the initial loss of cells and thus the decrease in impedance.

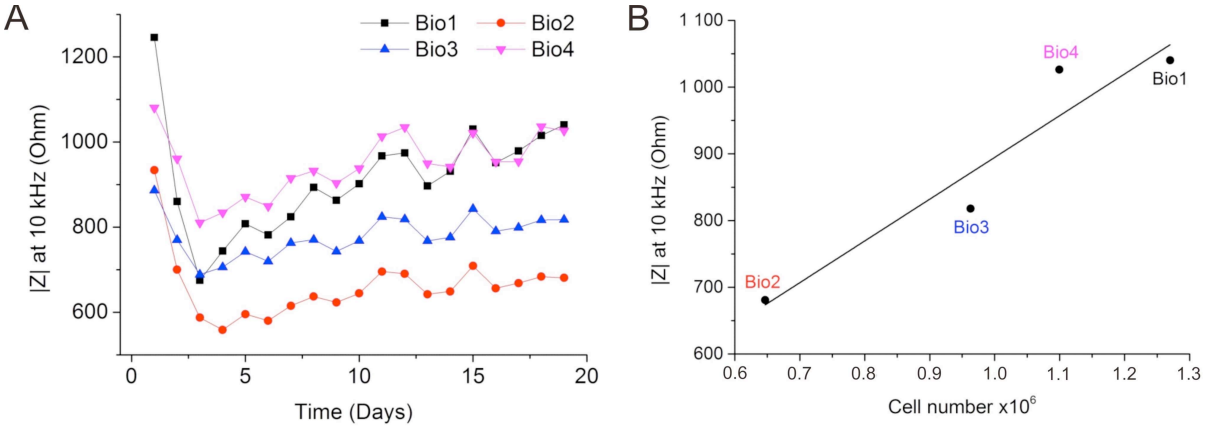

Figure 32. (A) Dynamic measurement of |Z| over 19 days of perfusion culture with HepG2 loaded bioreactors. (B) Linear correlation between the cell number found at day 19 and |Z| at 10 kHz (R^2 = 0.982).

4.1.3.5. Assessment of BAL function

Summary

RUG has had the main responsibility for this activity, working in close collaboration with DTU and Cellartis to evaluate the developed hiPSC-derived BALs. RUG moreover developed several versions of Liver-on-a-Chip array systems with integrated microelectrodes for oxygen sensing, enabling culture of six precision-cut liver slices (PCLS) simultaneously. Human PCLS (hPCLS) cultured in afore mention systems served as an *ex vivo* reference system for validating and assessing the developed hiPSC-derived BALs. The conditions for tissue culture (e.g. perfusion rate, oxygen transport, medium composition) was evaluated and optimised to allow culturing for 5 days. The BALs were characterized and analysed and the degree of differentiation of the hepatocytes produced from hiPSC appeared close to that of cultured human precision-cut liver slices with respect to functions and drug metabolism.

S&T results

Liver-on-a-Chip system for culturing hPCLS as ex vivo reference
Three versions of Liver-on-a-Chip systems have been developed during the course of the project. The 3rd and latest generation system is shown in **Fig. 33** and combines solutions for various problems that the 1st and 2nd generation systems had. First, sensor integration was simplified. Second, the time needed to open and close the chip during insertion of the PCLS was significantly shortened through use of a clamping system, the Micronit Fluidic Connect Pro. The two halves of the chips no longer need to be held together using 10 individually adjusted screws. This reduces the time during which the slices are exposed to atmospheric oxygen concentration considerably and the slice perifusion can be started immediately after slice loading, which improves tissue viability.

The size of the Liver-on-a-Chip (**Fig. 33**) was set for two side-by-side microscope slides (50 x 75 mm), featuring six individually addressable microchambers of 25µL volume each. At the in- and outlet of the chamber a combined WE/RE electrode can be reversibly attached using a fluidic connector. The device was connected to syringe pumps using standard 1/16" tubing or integrated with the micropumps used in the BAL support system (**Fig. 38Aa)**, a modular microfluidic control system incorporating peristaltic pumps, developed previously at DTU Nanotech. The footprint of the system complies with the SBS standard microtiter plate.

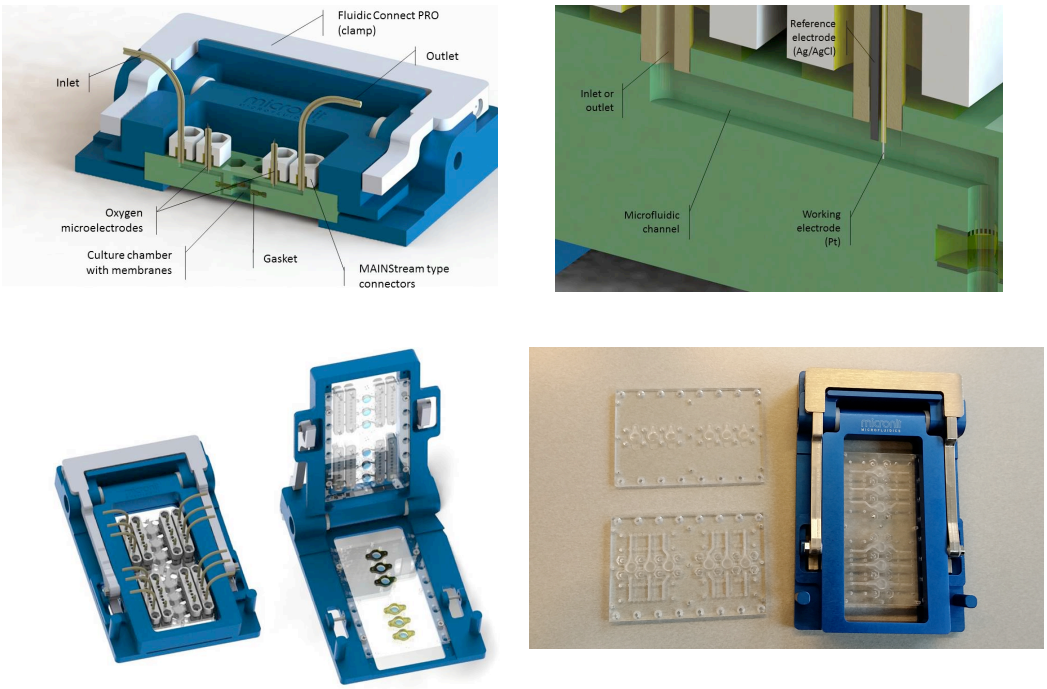

Figure 33. The 3rd-generation Liver-on-a-Chip inside the Micronit Fluidic Pro chip clamp. The upper left and right images are cross-sections, revealing the sensor inserts and fluidic part of the chip.

The Liver-on-a-Chip system was employed in a series of experiments using PCLS. Initially, a flow rate of 600 µL/h was employed for the perifusion, as was the case in previous set-ups. Although the logistics of the experiment itself improved substantially through the use of the chip holder, the viability of the incubated slices (as measured by ATP content) as shown in **Fig. 34** was lower than that observed in the well plates using this flow rate. An increase of the flow rate to 1200 µL/h appears to alleviate this.

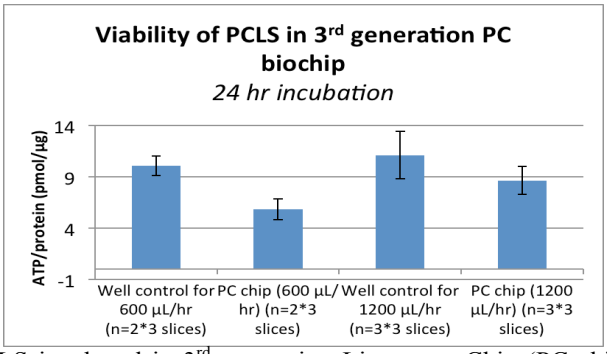

Figure 34. Viability of PCLS incubated in 3rd-generation Liver-on-a-Chip (PC chip) (24 h incubation), using different flow rates. Viability is expressed as the ATP content of the slice, normalized for its protein content. Levels between 10 and 12 pmol/µg are considered "normal" in well plates.

It was suspected that the lower viability of slices incubated using 600 µL/h compared to those incubated in well plates was a result of the absence of "re-equilibration" of the medium with oxygen from the surroundings of the chip, as was the case in one of the previously developed PDMS based

Liver-on-a-Chip system using the same flow rate. It was expected that the lower flow rate would result in less oxygen at the outlet of the device compared to 1200 µL/hr, as the residence time of the medium is longer and the slice would have more time to consume O_2.

After calibration at both 600 µL/h and 1200 µL/h flow rates, a PCLS was inserted in the culture well, and perifusion using 1200 µL/h flow rate was started. Measurement of medium oxygenation at both the in- and outlet was initiated immediately. After approximately 45 minutes, the flow rate was at once decreased to 600 µL/h, while the measurement was continued. In all cases, after an initial transition phase during which the slice was allowed to stabilize, a decrease of the oxygen concentration in the medium flowing out from the culture chamber could be observed after decreasing the flow rate. The result from a preliminary experiment is given in **Fig. 35**. From this it appears that a lower flow rate indeed results in a lower concentration of oxygen measured at the outlet, as was hypothesized based on the viability results and described above in **Fig. 34**.

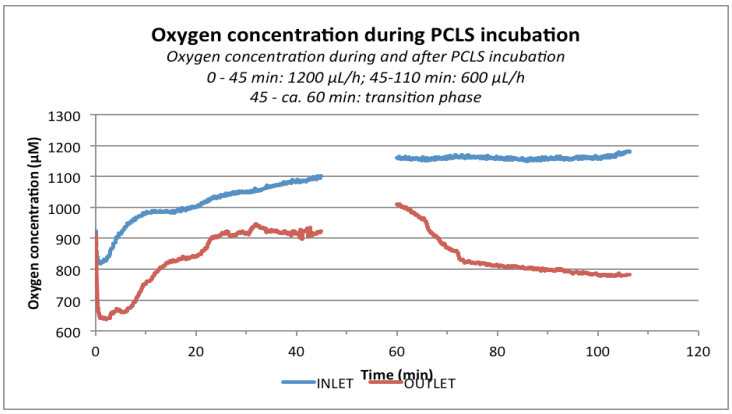

Figure 35. Oxygen concentration during PCLS incubation, measured at the in- and outlet of a 3rd-generation chip. Calibration of the sensors was done at 600 and 1200 µL/h flow rates. Initially, the slice is incubated at 1200 µL/h for ca. 45 minutes. After this period, flow rate was at once decreased to 600 µL/h. During this transition phase, no oxygen concentrations are depicted, as the slice needed to stabilize. The duration of the transition period is dictated by the overall volume of the fluidic part of the chip (approx. 75 µL), and the flow rate. At the new flow rate of 600 µL/h, the medium in the chip would be completely refreshed twice in 15 min.

Medium composition for liver slice culture

Experiments were conducted to assess the behaviour of human liver slices when incubated in different media. Both tissue function and metabolic activity were tested. Liver tissue was obtained from patients undergoing partial hepatectomy or from redundant parts of donor livers after split liver transplantation, and was approved by the Medical Ethical Committee of the University Medical Center Groningen. Four different types of media were tested on human liver slices: (1) WME (Williams Medium E, a serum-free medium originally developed for hepatocyte culture), (2) WME+ (WME with insulin, dexamethasone and serum), (3) RegeneMed (RegeneMed, Inc., developed for 3D liver cell culture, proprietary composition), (4) Cellartis (Cellartis medium optimized for maintenance culture of hepatocytes obtained by differentiation from hiPSC, proprietary composition).

Based on these tests, it became apparent that Cellartis medium in many instances performed better than the other media, with better maintenance of protein and ATP content, maintained Phase I metabolism for 5 days whereas it decreased in slices incubated in RegeneMed® and WME medium. The development of fibrosis/collagen deposition was observed in slices incubated in RegeneMed®, however this was seen to a much lesser extent in slices incubated in Cellartis medium. It was shown that hPCLS still contained substantial amount of glycogen (reflecting the function of the hepatocytes to store glucose in glycogen, a typical hepatocyte function) after 5 days of incubation in WME+, RegeneMed® and Cellartis media

Based on these results with human PCLS, it was decided to continue with Cellartis medium, the same medium as used for BAL perfusion.

Analysis of hiPSC-derived BAL at different conditions in comparison to PCLSs

Several BAL versions were created by DTU, using hiPSCs differentiated to the DE stage by Cellartis. The DE cells were produced from hiPSC by Cellartis and delivered to DTU. Scaffolds were prepared and loaded with hiPSC-derived DE cells and cultured for 25 days in the BAL support system with 16-bioreactor array at DTU. Two different scaffold designs (hexagonal and random**)** were tested and two flow rates (1 and 5 µL/min). The hepatic differentiation and functionality of hiPSC-derived hepatocytes were assessed at RUG using freshly obtained human PCLS as an *ex vivo* liver reference model. PCLS were incubated under static conditions in 12-well plates and in the liver-on-a-chip with a flow rate of 10 µL/min. Cells and slices were incubated in Cellartis hepatocyte maintenance culture medium.

The characteristics of these cells were determined with a palette of assays (metabolism, function, viability, and gene expression) developed by RUG. Human PCLS were cultured under static and flow conditions, using Cellartis hepatocyte maintenance medium. The same palette of assays was performed on the PCLS, static cultures and hiPSC-derived BALs. As the variation in liver function in the human population is well known to be large, the individual data of 3-9 human livers is given with the median value. The degree of hepatic differentiation in the BALs after 25 days of culture in Cellartis medium was analysed by gene expression of liver markers, albumin secretion and drug metabolism by phase I- and phase II activity.

An often used marker for hepatocyte function is albumin secreted into the medium. The medium from the respective BAL was collected and analysed using an ELISA kit. In regards to albumin, a similar or higher gene expression level (**Fig. 36**) was observed compared to the static references from Cellartis (dark blue bar) and DTU (yellow bar), which correlates with a lower expression of alpha-fetoprotein, i.e., the foetal form of albumin and should go from high to low during differentiation and maturation. The highest level of albumin expression was, however, seen for cultures in the Hex scaffold at a flow rate of 5 µL/min. The gene expression data for albumin were supported by a similar pattern in secretion level of albumin (**Fig. 37**) per scaffold for duplicate bioreactors and different conditions. Noteworthy is that the albumin secretion was increasing over time from day 21 to day 25.

The results show that albumin can be detected in the medium that passes through the BAL with the general trend that albumin secretion increases with time during the last day of differentiation, which is what should be expected.

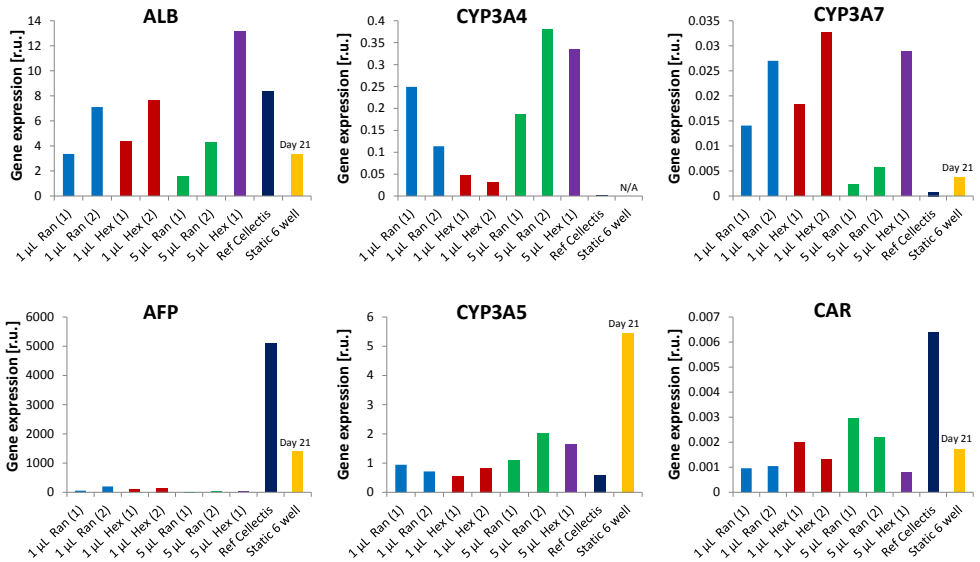

Figure 36. Effect of scaffold design and flow rate on gene expression of hepatocyte specific markers: hiPSC-derived DE cells were cultured and hepatic differentiated inside a 3D random porous scaffold (Ran) or a combined structured/random porous scaffold (Hex) at perfusion conditions at a flow rate of 1 µL/min or 5 µL/min for 25 days. Each culture condition was performed in duplicate and is shown in the diagrams as separate bars to easily visualize variation between parallel cultures at the same condition and easy comparison of gene

expression of the same bioreactor culture to albumin secretion (Fig. 4.23) and phase I and phase II activity (Fig. 4.24), which are all shown in the same order in the diagrams. Gene expression was analyzed by qRT-PCR using Taqman® assays for the genes: Albumin (ALB), alpha-fetoprotein (AFP), CYP3A4, CYP3A5, CYP3A7, and constitutive androstane receptor (CAR). Gene expression is normalized to expression of CREB-binding protein. Two 2D static references are included: One based on cDNA from cells cultured at Cellartis (Ref Cellartis) and another based on cells cultured at DTU for 21 days in a standard 6 well plate (Static 6 well).

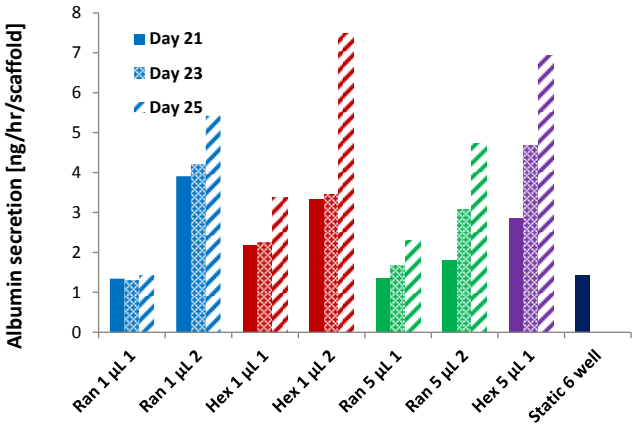

Figure 37. Effect of scaffold design and flow rate on albumin secretion: hiPSC-derived DE cells were cultured and hepatic differentiated inside a 3D random porous scaffold (Ran) or a combined structured/random porous scaffold (Hex) at perfusion conditions at a flow rate of 1 µL/min or 5 µL/min for 25 days. Each culture condition was performed in duplicate and is shown in the diagrams as separate bars to easily visualize variation between parallel cultures at the same condition and easy comparison of albumin secretion of the same bioreactor culture to gene expression (Fig. 4.22) and phase I and phase II activity (Fig. 4.24), which are all shown in the same order in the diagrams. Medium from the BAL outlets were collected at day 21, day 23, and day 25 and analyzed for albumin by ELISA (E80-129, Bethyl Laboratories).

A very important test for BAL function is the ability to metabolise drugs. This was done by adding test substrates to the perfusion medium and measuring the metabolite using HPLC or mass spectrometry. The BAL was first matured and then perfused with 7-ethoxycoumarin (phase I and II metabolism) or 7-hydroxycoumarin (phase II metabolism). The medium for the respective BALs was collected after the BAL was filled with medium containing the respective forms of coumarin. The medium was then frozen and shipped to P5 for HPLC analysis. The results are shown in **Fig. 38** where addition of the coumarin substrates showed the highest metabolic activity with respect to glucuronidation and sulfation at the highest flow rate, 5 µL/min, and at a level similar or higher than for liver slice cultures. Furthermore the glucuronidation activity was, as expected, higher than the sulfation activity.

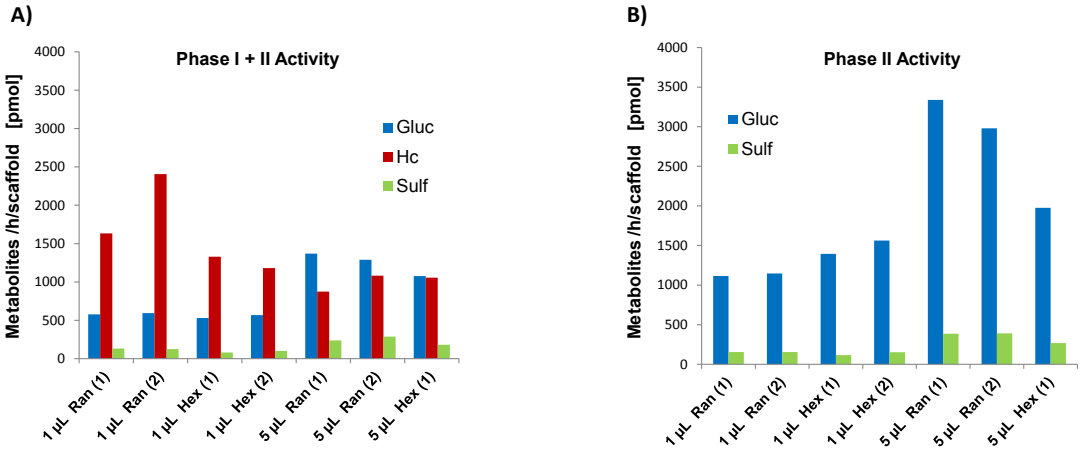

Figure 38. Effect of scaffold design and flow rate on phase I- and Phase II activity: hiPSC-derived DE cells were cultured and hepatic differentiated inside a 3D random porous scaffold (Ran) or a combined structured/random porous scaffold (Hex) at perfusion conditions at a flow rate of 1 µL/min or 5 µL/min for 25 days. Each culture condition was performed in duplicate and is shown in the diagrams as separate bars to easily

visualize variation between parallel cultures at the same condition and easy comparison of phase I and phase II activity of the same bioreactor culture to gene expression (Fig. 4.22) and albumin secretion (Fig. 4.23), which are all shown in the same order in the diagrams. For the activity experiments, the scaffolds were removed from the flow bioreactor and placed in a 48 well plate in 1 mL medium with the added specific substrate(s). The scaffolds were then incubated for 2½ hours at 37°C/5% CO_2 and medium collected and stored at -20 °C for later analysis of metabolites by HPLC. A) For phase I and phase II activity measurements, the medium was added 500 µM 7-ethoxycoumarin and analyzed for the metabolites Gluc: 7-hydroxycoumarin glucuronide, Hc: 7-hydroxycoumarin, and Sulf: 7-hydroxycoumarin sulphate. B) In case no phase I activity would take place, 500 µM 7-hydroxycoumarin (product in phase I, and substrate for phase II activity) was added to the medium in another experiment, but to the same scaffolds. The medium was analyzed for the metabolites Gluc: 7-hydroxycoumarin glucuronide and Sulf: 7-hydroxycoumarin sulphate.

Expression of different hepatic genes responsible for liver development, synthesis, metabolism and membrane transport in hiPSC-derived BAL differentiated under different conditions and in PCLS were compared. The expression of the foetal liver marker AFP was lower in hiPSC-derived BAL cultured under flow compared to static cultures, but was higher than in PCLS, where it was nearly absent. This indicates the beneficial effect of flow on hepatocyte maturation. Expression of CYP3A7 (also mainly expressed in foetal liver) was low and similar to PCLS in all cell culture conditions. Expression of hepatic nuclear factor, HNF4α (liver differentiation marker), and nuclear receptor, CAR, which both regulate the expression of many hepatic genes, showed different expression patterns. HNF4α showed good expression levels, whereas CAR was poorly expressed hiPSC-derived BALs cultured under all conditions compared to liver slices. Different CYP enzymes showed different expression levels. For example, CYP3A5 was expressed more in hiPSC compared to PCLS, on average 4-to 5-fold higher for hiPSC cultured at 5µL/min flow, and 9- to 12-fold higher in hiPSC cultured under static condition. On the other hand, CYP3A4 and CYP2B6 had low expression in hiPSC-derived BAL compared to hPCLS.

Overall the data indicates that hiPSC-derived BAL differentiate under flow into both hepatic and biliary directions, as epithelial biliary cell markers, such as CK7 and BGP, were well expressed in cell cultures.

Assessment of BAL function in comparison to hPCLSs

The final assessment of the hiPSC-derived BAL was performed by determining phase I metabolism for individual CYP enzymes by incubation of the BALs and hPCLS with a cocktail of substrates specific for different isoforms of CYP. The results showed different activity levels compared to hPCLS. It is very important to realize that the metabolic activity of human livers shows a large inter-individual variation, and that the number of human donor livers for slices and number of donors for stem cells are limited. Therefore we draw conclusions about cell differentiation by comparing the range of activities rather than the average or the median values.

Production of metabolites of midazolam, a substrate for CYP3A4 enzyme, reaches similar levels in hiPSC-derived BAL as PCLS under static conditions (**Fig. 40**). This is a truly important finding, as up to now CYP3A4 activities in differentiated hiPSCs did not reach these levels. However in both hPCLS and hiPSC-derived BALs, the values were higher in static cultures than under flow conditions. One possible explanation is that under flow conditions the hPCLS and hiPSC-derived hepatocytes are cultured in devices/scaffolds made of PDMS, a material, which is known for its high absorption of mainly lipophilic compounds. Midazolam, the substrate used for CYP3A4, is a highly lipophilic compound, and absorption may reduce the free concentration and therefore the metabolic rate. It is also noteworthy that the hiPSC-derived hepatocytes have activity comparable to the hPCLS in PDMS. This phenomenon may also be relevant for other substrates but to a different extent. CYP1A, CYP2D6 and CYP2C19 activities in static cultures were shown to be in the range of the liver samples but all in the lower part of this range. CYP2B6 and CYP 2C9 activity of cells was shown to be low for all conditions compared to PCLS. For the majority of tested CYP enzymes, the 5µL/min flow rate exhibited a better effect on enzyme activities compared to the 1 µL/min flow rate. There was no clear difference between hexagonal and random scaffolds.

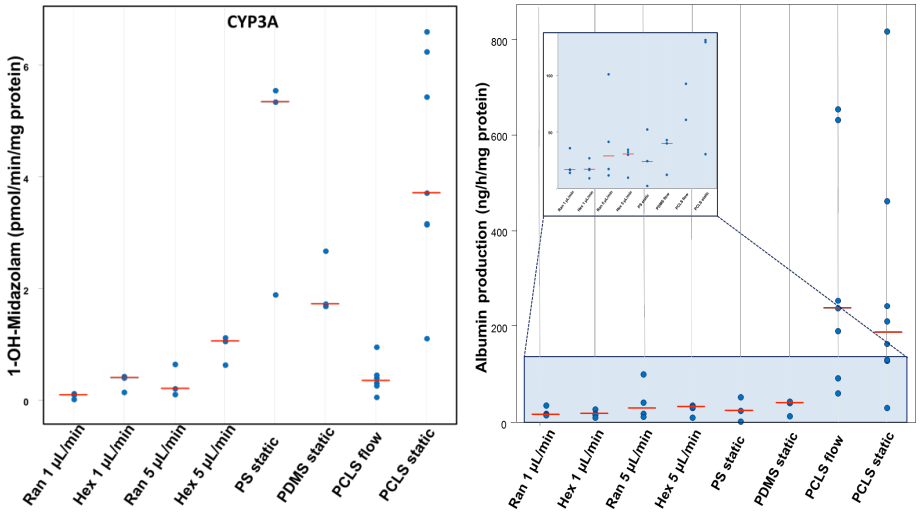

Figure 40. Cytochrome P450 3A4 activity (*left*) and albumin production (*right*) of the BAL differentiated and matured under static or flow conditions and with different scaffold structure (*right*) as compared with PCLS derived from 7 human livers, resulting in a very good overlap in function.

Phase II metabolism was tested with 7-hydroxycoumarin as substrate. Differentiated cells exhibit uridine 5'-diphospho-N-acetyltransferase (UGTs) and sulfotransferase (SULT) activities. Surprisingly, 7-HC-G production by cells cultured at 5µL/min flow in both hexagonal and random scaffolds was on average twofold higher than in liver slices, whereas sulfation rates of 7-HC were 30- to 40-fold higher than in PCLS cultured under flow. 7-HC-S production in static cultures was equal to that in liver slices cultured under static conditions. Glucuronidation rates, however, were 30-40% of the 7-HC-G production in hPCLS cultured under static conditions. Cells that were differentiated and cultured at 1 µL/min flow rate exhibited lower levels of metabolite production compared to 5µL/min flow. Nevertheless, the 7-HC conjugate production by hiPSC-derived BAL was still similar or higher compared to liver slices; 7-HC-G production was 50-90% of that of the hPCLS, while 7-HC-S production was 20-fold higher than that of the hPCLS.

Bile secretion by the hiPSC-derived BAL was at the same level in cells differentiated under static conditions for 22 days or 24 days as in PCLS. We could not detect bile acids in samples of outflow medium obtained under flow conditions, probably due to the high dilution rates that are a consequence of perfusion. On average, urea production by hiPSC-derived BAL was lower compared to that of liver slices. BALs differentiated at 5 µL/min flow and under static conditions showed higher urea synthesis than those differentiated at 1 µL/min flow. However, as with albumin production, some of the values obtained from BAL cultures were on the same level as the lowest values of the human donors.

4.1.3.6. Conclusion

This is the first time that the function of hiPSC-derived hepatocytes or BALs has been compared to fresh human tissue. Moreover, it reveals that these hiPSC-derived hepatocytes, cultured on the developed 3D scaffolds under perfusion into a BAL, show as yet unrivalled functionality, with excellent comparability of liver functions with fresh liver tissue. The differentiation of hiPSC-derived hepatocytes under flow conditions in the scaffolds was similar to that in normal cultures, realizing this unique possibility to differentiate and mature cells directly in a perfusion based support system. Overall the achievements in NanoBio4Trans were possible due to excellent collaborative and cross-disciplinary efforts of all the partners.

4.1.4. Impact, exploitation and dissemination

4.1.4.1. Impact

We expect NanoBio4Trans to have a strong impact in the following main areas: (1) medical technology, e.g., tissue engineering, regenerative medicine, artificial organs, (2) scientific fields such as nanotechnology, sensors, material science, and cell biology, (3) development of high-tech SMEs, but most of all, the health and quality of life of patients with liver diseases. The prevalence of liver diseases is estimated to be approximately 6% in the EU. Among the 490 million EU inhabitants, this equates to some 29 million people. Mortality rates from chronic liver diseases across the European region vary widely from 53.6 persons per 100.000 in Hungary to 4.4 per 100.000 in the Netherlands. The mortality rate for chronic liver diseases was estimated at 14.3 per 100.000 in the EU in 2004, making it the fifth most common cause of death in the EU. This means that more than 70,000 Europeans are dying from chronic liver diseases every year. Aging population and increase in obesity and nonalcoholic fatty liver (NAFL, 30% in the general population in Europe), which can lead to non-alcoholic steatohepatitis (NASH, 10-20 % of NAFL) and cirrhosis, end-stage liver disease, and hepatocellular carcinoma means that liver diseases will be a major challenge to healthcare systems in the near future. It is quite possible that NAFL will become the most common cause of advanced liver disease and liver failure in the 21st century. The World Health Organization estimates that 10% of the world's population has chronic liver disease and that liver cirrhosis will be the ninth most common cause of death in the western world by 2015.

Expected impact of HEALTH.2012.1.4-2	**Expected results of NanoBio4Trans**	**Result achieved**
" Results should lead to development of new tools, technologies or devices for use in transplantation….."	**New technology** for mass production and differentiation of hiPSC. These hiPSC can be use in BAL, for cell replacement therapy or for stem cell transplantation.	1. hiPSC production has been scaled up through 3D culturing in spheroid (hepatospheres) cultures. 2. hiPSC-derived hepatocytes, hepatosphere and their progenitors have been used to develop BALs with as yet unrivalled functionality, with excellent comparability of liver functions with fresh liver tissue.
	New advanced monitoring **tools,** biosensor systems, **and devices** for assessing liver function. This can be used for further development and quality control of **BAL for extracorporeal use or for transplantation**	1. Electrochemical sensors for monitoring oxygen levels in tissue culture array chips 2. Bioimpedance sensors for monitoring growth of tissue and bioartificial organs (BOs) 3. Optical sensors for monitoring extracellular and intracellular oxygen and pH levels in cells tissues and BOs 4. A palette of assays to conduct gene expression-, metabolic and functional test on BALs and liver tissue. 5. BAL support system for growth of up to 16 BALs and potentially other BO

	New highly parallelized microfluidic BAL-on-a-Chip devices with integrated imaging tools for high-throughput optimization and metabolic investigations of hiPSC, progenitor cells and hepatocytes	1. Multi-channel BAL-on-a-Chip (16 channels) and Liver-on-a Chip (6 channels) devices with integrated electrochemical sensing and potential for future impedance tomography imaging of BAL. 2. Validated and assessed BAL support system for culturing hiPSCs into state of the art functioning BALs under perfusion control and indication that spheroid cultures could favourably be used instead of cells alone. 3. Phosphoroscent and fluoresencent O_2 and pH nanoprobes has successfully been used for imaging of various tissue
"…and for replacing essential organ function by bioartificial organs."	Replacing essential organ function by extracorporeal BAL	Future tests to be conducted

Liver transplantation has become a lifesaving procedure for patients who have chronic end-stage liver disease and acute liver failure. The gap between patients waiting for an organ and those actually receiving one widens each year, leading to longer waiting times (currently ~11000 patients in EU, where ~22% die while waiting), frequent recipient hospitalizations, and sicker candidates with less favourable recipient outcomes. In the EU ~6500 liver transplantations are conducted/year, each at the cost of ~230k€ with a follow-up charge of ~17k€/year, a large fraction related to immune suppressive medication. It is obvious that bioartificial livers (BALs) and extracorporeal bioartificial livers (EBALs) can have very important impact in this context.

New tools, technologies or devices for use in transplantation
New technology for mass production of hiPSC and for differentiating hiPSC to progenitor cells and hepatocytes have been achieved. These cells and hepatospheres could potentially be used in an EBAL, and in the long term for implantable BAL, as outlined in **Fig. 41**, however obviously first after vigorous testing for cellular safety. With this in mind, this technology could also deliver cells for cell transplantation and progenitor cell therapy for liver regeneration as potential alternative to liver transplantation. Repopulating the damaged liver is the key goal of progenitor cell therapy for liver failure. hiPSC may be a most attractive cell type for this purpose, as they can be taken directly from the patient, and do not carry the ethical concerns of embryonic stem cells. For human therapy it will be necessary to apply a quantity of cells well over 5 % of the liver mass, however it is questionable if the approach in NanoBio4Trans will approach such quantities in an very near future. We have taken important steps towards developing technology for mass production and differentiation of hiPSC into DE cells, hepatocytes and hepatospheres, but progenitor cell therapy has been beyond the scope of NanoBio4Trans.

Replacing essential organ function by bioartificial organs
The final goal of NanoBio4Trans has been to have an optimised and validated vascularised BAL, ready to be perfused with human blood plasma from a liver-deficient donor, at first as an extracorporal liver. Such an **EBAL** can **support** or **replace liver function** temporarily to prevent or reverse secondary organ failure complications and to promote restoration of native liver function through regeneration. Additionally, it may provide the crucial bridge for survival to transplantation with a suitable donor liver. NanoBio4Trans has indeed developed an optimised vascularised BAL, ready to

be perfused with plasma, that has been evaluated using human liver tissue as an ex vivo reference model, with results indicating that its behaviour and function is close to and similar to that of real human liver tissue. However its applicability as an EBAL needs to be studied and confirmed by continued and future experiments.

The use of hiPSC technology for making an EBAL could be developed further towards a more *personalised* BAL for transplantation and thus possibly eliminate the need for immune-repressive drug treatment in the future (see **Fig. 41**). However, it will very likely take several weeks to grow sufficient amounts of hiPSC from patients´ own cells and for the further differentiation into progenitor cells and hepatocytes. Therefore, there will still be a need for EBALs as crucial bridge for survival to transplantation.

The impact on health economy and society will be tremendous since its realisation could save ~100M€ /year alone on immunosuppressive treatment, assuming reduced rejection issues with hiPSC-derived BALs. While NanoBio4Trans has focused on liver transplantation, the technology could be applied to other organs, increasing the commercial potential and health and economic impact even further. The project has developed entirely new tools that can be used in the pharmaceutical industry for testing new drugs, toxicity and therapies on human-like patient specific material, which can help fill the gap between pre-clinical and clinical trials. Moreover other bioartifical organs (BO) and BO-on-a-Chip systems could be developed based on the same technology, as also indicated by the successful differentiation of Cellartis hiPSCs into lung- and beta cell progenitors.

4.1.4.2. Exploitation

The ultimate goal of the BAL technology is to bring the technology to the clinics to save patient's lives, society's money and avoid unethical treatments, such as transplant tourism. Although NanoBio4Trans may have identified some limitations for BAL size, a number of components, e.g., cell availability, pump systems, might be limiting in the current experimental system, but they may not be real in a future industrialised setting addressing larger BALs. It should be noted that the NanoBio4Trans BAL is not yet a stand-alone extracorporeal liver, but will rely on support systems that clear the plasma/blood for some of the toxic substances before reaching the BAL. The scheme below presents the "time-line" for the project during its lifetime, and beyond (**Fig. 41**), where we have reached all results and achieved all milestones that were anticipated.

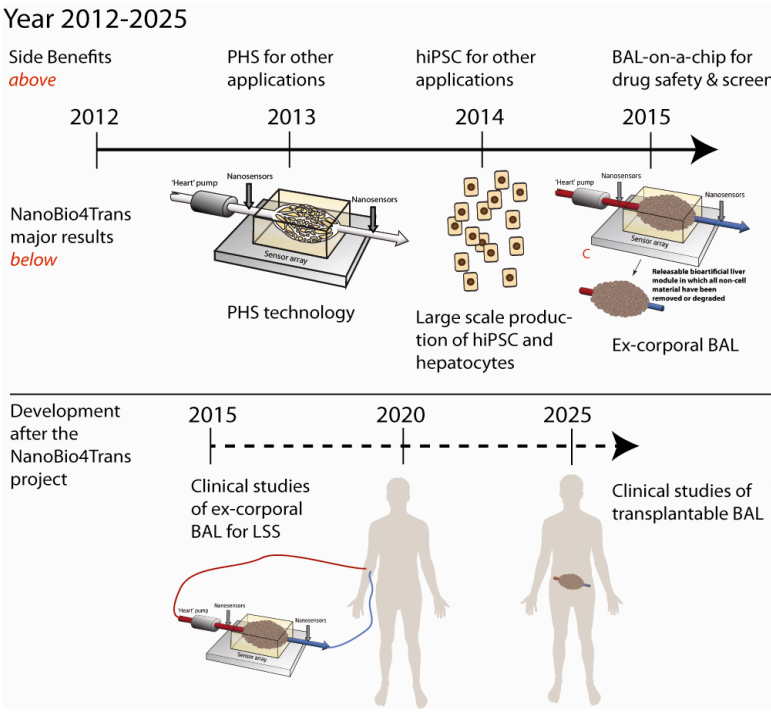

The NanoBio4Trans consortium has analysed all possible outcome of the project, their possible novelty, transfer, and exploitation. This activity was carefully coordinated by the participating SMEs, and a preliminary exploitation plan was created. SMEs are by nature, component providers to BAL and similar BO. After the BAL development achieved during the lifetime of this project, other projects must take over the RTD outcomes, to bring the NanoBio4Trans BAL first, to clinical trials and then, to the market. Obviously the three SME involved in NanoBio4Trans, are expected to be highly active as future component providers, which is well in-line with their individual business plan.

However, when considering commercialising BALs and BOs, other companies might be better suited for this task. It is foreseen, that a large infrastructure is needed to be able to maintain BALs for day-to-day delivery, suggesting that a larger company might be a better match. An established global company with good clinical connection, like Gambro AB, Lund Sweden (already providing dialysis system for kidney and liver patients), would probably be a good choice for commercialising the complete BAL systems.

Due to its novel, trans-sectorial, complementary, and synergetic approach, NanoBio4Trans has generated intellectual property both at SME and University levels. IPR is sought protected through 3 patents (2 granted and 1 in the application phase). The patents will be used to try to attract financing from a global company commercialising BALs and/or venture capital. The IPR will actively be pursued also at the Universities in order to increase the attractiveness for the BAL technology for investors, participating SME and future collaborating companies.

Furthermore at our Exploitation Strategy Seminar we identified a number of interesting exploitable results (confidential), which may be relevant to exploit further from a commercial point of view. At this point the Consortium considers the finding to be important advancements of knowledge.

As indicated in **Fig. 41,** it is foreseen that a clinical grade BAL could arrive to the market around 2025. However, it is plausible that a large commercialisation boast of BAL-related technologies could result in the use of the technology for other purposes already in a much nearer future 2017-2018. Furthermore, the tools developed in NanoBio4Trans are generic and can be used to a large extent in other projects with the goal to provide other types of BOs, like kidneys, hearts and intestines. Is it therefore reasonable to expect that the PHS could be commercialised for other applications besides BAL. Likewise, large scale production of blood type, and if needed HLA specific hiPSC will simplify usage of this ethically appealing source of stem cells in science and medicine. Sensor systems can be used for many more purposes and can be applied in basic research in many fields. As such, NanoBio4Trans can serve as a nucleation site for many branched activities in the BO field and biomedical sciences. The next step foreseen to follow the commercialisation of basic technologies (sensors, PHS and blood type specific hiPSC), is the exploitation of the BAL-on-chip systems in drug development/pharmaceutical industry.

4.1.4.3. Dissemination

The main dissemination activities in the NanoBio4Trans have been oral and written presentations of research results to the scientific community. Other dissemination activities have included e.g. newspaper articles (Denmark and Sweden), presentation of research results to civil society at Researchers Night in Denmark in 2014 and a NanoBio4Trans video which has been shown at our public event in Milano, Italy in May 2015 to an audience of researchers, people from industry and medical doctors, incl. in the Department of Micro- and Nanotechnology newsletter Sept. 2015, and published on YouTube August 2015 (https://www.youtube.com/watch?v=PCmWOUiZRHA).

Means of dissemination	**Number**
Peer reviewed journal articles published	22
Peer reviewed journal articles submitted or in manuscript	6
Peer reviewed proceedings	23
Book chapters	5
Reviews	3
Posters	34

Oral presentations (whereof > 15 as invited speaker)	38
Patents/patent applications	3
Newspaper articles/interviews	3
Articles/interviews in specialist magazines	1
Public event	1
Videos	1

A successful public event was held in Milano, Italy, in May 2015 in cooperation with the FP7 funded project D-liver (http://www.d-liver.eu/). The event was held at a hospital in Milan, Italy, with 50 participants. The joint event secured dissemination and outreach to relevant potential partners and end-users, e.g. medical doctors.

4.1.5. Project website

http://www.nanobio4trans.eu/